Development/Plasticity/Repair

The Wnt Adaptor Protein ATP6AP2 Regulates Multiple Stages of Adult Hippocampal Neurogenesis

Simon T. Schafer,[1,2,3] Jinju Han,[1] Monique Pena,[1] Oliver von Bohlen und Halbach,[3] Jörg Peters,[2]* and Fred H. Gage[1]*

[1]Laboratory of Genetics, The Salk Institute for Biological Studies, La Jolla, California 92037, [2]Institute of Physiology, University of Greifswald, 17495 Karlsburg, Germany, and [3]Institute of Anatomy and Cell Biology, Universitätsmedizin Greifswald, 17487 Greifswald, Germany

In the mammalian hippocampus, canonical Wnt signals provided by the microenvironment regulate the differentiation of adult neural stem cells (NSCs) toward the neuronal lineage. Wnts are part of a complex and diverse set of signaling pathways and the role of Wnt/Planar cell polarity (PCP) signaling in adult neurogenesis remains unknown. Using *in vitro* assays on differentiating adult NSCs, we identified a transition of Wnt signaling responsiveness from Wnt/β-catenin to Wnt/PCP signaling. In mice, retroviral knockdown strategies against ATP6AP2, a recently discovered core protein involved in both signaling pathways, revealed that its dual role is critical for granule cell fate and morphogenesis. We were able to confirm its dual role in neurogenic Wnt signaling *in vitro* for both canonical Wnt signaling in proliferating adult NSCs and non-canonical Wnt signaling in differentiating neuroblasts. Although LRP6 appeared to be critical for granule cell fate determination, *in vivo* knockdown of PCP core proteins FZD3 and CELSR1-3 revealed severe maturational defects without changing the identity of newborn granule cells. Furthermore, we found that CELSR1-3 control distinctive aspects of PCP-mediated granule cell morphogenesis with CELSR1 regulating the direction of dendrite initiation sites and CELSR2/3 controlling radial migration and dendritic patterning.

The data presented here characterize distinctive roles for Wnt/β-catenin signaling in granule cell fate determination and for Wnt/PCP signaling in controlling the morphological maturation of differentiating neuroblasts.

Key words: **adult neurogenesis; ATP6AP2; CELSR1-3; PCP signaling; Wnt signaling**

Introduction

Neurogenesis in the adult mammalian nervous system is restricted to the subventricular zone (SVZ) of the lateral ventricles and the subgranular zone (SGZ) of the dentate gyrus (DG; Gage, 2000; Alvarez-Buylla and Lim, 2004). New neurons are continuously generated from neural stem cells (NSCs) that undergo distinct developmental steps, including proliferation, differentiation, migration, and dendritic targeting (van Praag et al., 2002; Ge et al., 2007; Ming and Song, 2011; von Bohlen und Halbach, 2011).

ATP6AP2, an accessory subunit of the vacuolar (V)-ATPase, plays essential roles during development and has been shown to be a crucial component in promoting canonical Wnt and non-canonical Wnt/PCP signaling (Buechling et al., 2010; Cruciat et al., 2010; Hermle et al., 2013). Wnt signaling, in particular its canonical branch, has been shown to be instrumental in several aspects of adult hippocampal neurogenesis. Canonical Wnt/β-catenin signaling is initiated upon formation of a tertiary complex that includes the receptor FZD (frizzled), its coreceptor LRP6 (low-density lipoprotein receptor-related protein 6) and a soluble Wnt ligand, such as WNT3A, that is produced by local hippocampal astrocytes (Song et al., 2002; Lie et al., 2005; Kuwabara et al., 2009). In cooperation with ATP6AP2, the FZD:LRP6:WNT3A complex triggers the formation of a signalosome at the plasma membrane, internalizing the whole complex to further transduce the signal (Blitzer and Nusse, 2006; Yamamoto et al., 2006; Bilic et al., 2007; Cruciat et al., 2010; Niehrs, 2012). Eventually, β-catenin becomes stabilized and translocates into the nucleus, acting as a transcriptional coactivator of TCF/LEF (T-cell-specific transcription factor/lymphoid enhancer binding factor) transcription factors. The proneurogenic factors *Prox1* and *Neurod1* are among the major direct transcriptional targets of Wnt/β-catenin-TCF/LEF signaling in NSCs and are known to control genes specifically involved in neuronal differentiation (Gao et al., 2009; Kuwabara et al., 2009; Lavado et al., 2010; Karalay et al., 2011).

In addition to canonical Wnt signaling, non-canonical Wnt/Planar cell polarity (PCP) signaling is the most extensively studied pathway among the several non-canonical pathways that do not involve β-catenin. It is essential for orienting and polarizing

Received Oct. 6, 2014; revised Feb. 18, 2015; accepted Feb. 22, 2015.

Author contributions: S.T.S., O.v.B.u.H., J.P., and F.H.G. designed research; S.T.S., J.H., and M.P. performed research; S.T.S., J.H., M.P., O.v.B.u.H., J.P., and F.H.G. analyzed data; S.T.S. wrote the paper.

This work was supported by the German Research Foundation (PE 366/12-1 and BO 1971/6-1), the James S. McDonnell Foundation, the JPB Foundation, The G. Harold and Leila Y. Mathers Foundation, The Leona M. and Harry B. Helmsley Charitable Trust (2012-PG-MED002), NIH Grant MH090258, and a fellowship to S.T.S. from the German National Academic Foundation. We thank Dr J. Mertens for the pLVXEP plasmid, Drs J. Mertens and A. Denli for discussions and suggestions, and M. L. Gage for editorial comments.

*J.P. and F.H.G. are co-senior authors.

The authors declare no competing financial interests.

Correspondence should be addressed to Simon Thomas Schafer, Laboratory of Genetics, The Salk Institute for Biological Studies, 10010 North Torrey Pines Road, La Jolla, CA 92037. E-mail: sschafer@salk.edu.

DOI:10.1523/JNEUROSCI.4130-14.2015

 0270-6474/15/354983-16$15.00/0

cells in the plane of a tissue. Directional signals are processed through PCP core components such as FZD, DVL (Dishevelled), CELSR (Cadherin EGF LAG seven-pass G-type receptor), VANGL (van Gogh-like), and Prickle to establish planar polarity within individual cells (Tissir and Goffinet, 2013). Downstream effectors, such as small GTPases, convert these signals into morphogenetic programs by rearranging the cytoskeleton and inducing the expression of target genes (Schlessinger et al., 2009). Although recent studies on the PCP core proteins CELSR1-3 and FZD3 revealed essential functions in dendritic patterning, axonal tract development, neuronal migration, and hair cell orientation (Shima et al., 2007; Qu et al., 2010; Feng et al., 2012a), it remains unknown whether different canonical and non-canonical Wnt signals act in a stage-specific manner to regulate distinctive steps of adult hippocampal neurogenesis. Here we identified a maturational signaling transition from canonical to non-canonical Wnt/PCP signaling in which the non-canonical Wnt/PCP signaling pathways appeared to be indispensable for proper morphological maturation and integration of adult-born granule cells into the DG.

Materials and Methods

Plasmids and viruses. For ATP6AP2 overexpression, full-length rat *Atp6ap2* cDNA was subcloned into the pLVXEP vector (a gift from Dr Mertens, Salk Institute for Biological Studies) containing an elongation factor 1 (EF1)α promoter. The ΔECD mutant lacks amino acids 1–265 of the extracellular domain. Non-overexpressing control cells were transfected with the pLVXEP vector only. HA-tagged CELSR2- and 3-expressing plasmids pEF-CELSR2-HA and pcDNA-CELSR3-HA (a gift from Dr Uemura, Kyoto University, Japan) were used for localization experiments in differentiating adult hippocampal progenitor cells (AHPs). FLAG-tagged ATP6AP2, corticotropin-releasing hormone receptor (CRF) and FZD3-expressing constructs were generated by subcloning the respective mouse cDNAs into the pCK vector (a gift from Dr. V. Narry Kim). For the retroviral experiments, shRNAs targeting mouse and rat genes respectively were cloned into a retroviral construct containing a chicken β-actin (CAG)-driven green fluorescent protein (GFP) and a hU6 promoter driving expression of shRNAs, as described previously (Zhao et al., 2006). As a control, we used a target sequence not matching to any rodent mRNA sequence. Knockdown efficiencies were confirmed by transfection of mouse Neuro-2A cells (ATCC), as well as primary rat hippocampal AHPs using qRT-PCR and Western blot. Retroviruses were produced as previously described (Zhao et al., 2006). Titers ranged from 2 to 5×10^7 colony forming units/ml.

Cell culture. The isolation, characterization, and culturing of AHPs used in this study were previously described (Palmer et al., 1997). Proliferating AHPs were cultured in serum-free media, DMEM-F12 (glutamine) containing N2 supplement and 20 ng/ml FGF-2 (PreproTech). For neuronal differentiation, AHPs were transferred into medium containing 1 μM retinoic acid (Sigma-Aldrich) and 5 μM forskolin (Sigma-Aldrich) for the indicated number of days.

Primary astrocytes were isolated from rat hippocampi and cocultured with AHPs (Song et al., 2002). AHPs were plated on a confluent astrocyte feeder layer in serum-free conditions.

Luciferase assays. For dual luciferase assays, AHPs were electroporated with the following reporter plasmids using a nucleofector device (Amaxa): Super8xTOPFLASH (with TCF/LEF binding motifs), Super8xFOPFLASH (mutant motif), pAP-1-luc (PathDetect *cis*-reporting system from Stratagene), and Renilla-Luc under the control of the human cytomegalovirus promoter as internal control. Cells were treated with 50 ng/ml WNT3A (R&D Systems), 50 ng/ml WNT5A (R&D Systems), or 250 mM CHIR99021 (LC Laboratories) in the absence of differentiating factors for 24 h at the time points indicated. Luciferase activity was then measured using the Dual-Luciferase Reporter Assay System (Promega).

Stereotactic injections. All animal procedures were done in accordance with protocols approved by the animal care and use committee of The Salk Institute for Biological Studies. For retroviral loss-of-function experiments, 6- to 7-week-old female C57BL/6 mice were used (Harlan); they were kept under a constant 12 h light/dark cycle. Stereotactic injections of 1 μl of retroviral suspension were placed into the DG (coordinates from bregma: -2 anterioposterior, ± 1.5 mediolateral, -2.3 dorsoventral). Group sizes for all experimental groups were $n \geq 3$.

Immunostaining and in situ *hybridization.* Animals were anesthetized with ketamine/xylazine and then transcardially perfused with a 0.9% NaCl solution followed by 4% paraformaldehyde (PFA) in 0.1 M phosphate buffer, pH 7.4. Brains were removed, postfixed overnight at 4°C and then transferred into 30% sucrose solution for cryoprotection. Forty-μm thick coronal sections were obtained using a sliding microtome (Leica) and subjected to immunohistochemistry as previously described (Jessberger et al., 2008). Primary antibodies used were chicken α-GFP (1:500; Aves), goat α-DCX (1:250; Santa Cruz Biotechnology), mouse α-Prox1 (1:250; Millipore), goat α-Sox2 (1:250; Santa Cruz Biotechnology), rat α-FZD3 (1:500; R&D Systems), and rabbit α-Sox2 (1:250; Cell Signaling Technology). Secondary antibodies were all obtained from Jackson Immunoresearch.

Immunohistochemistry was performed on cultured cells fixed with 4% PFA for 30 min followed by extensive washes in phosphate buffer. The following primary antibodies were used: rabbit α-Tuj1 (1:1000; Covance), rabbit α-HA (1:500; Sigma-Aldrich), mouse α-β-catenin (1:500; Cell Signaling Technology), goat α-Sox2 (1:250; Santa Cruz Biotechnology). For *in situ* hybridization, mouse brains were cryosectioned into 12-μm-thick coronal sections and treated with 4% PFA for 10 min and 0.25% acetic anhydride for 10 min. The *Celsr1*, *2*, and *3* cDNAs were subcloned into the pBluescript vector (Addgene) using previously described primers (Tissir et al., 2002). RNA sense and antisense probes were synthesized using T3 or T7 RNA polymerase (Promega). After prehybridization, sections were incubated overnight at 58°C with digoxigenin-labeled RNA probes in hybridization buffer (Ambion). Slides were washed twice with 5× SSC (Invitrogen) and 0.2× SSC before incubation with the alkaline-phosphatase antibody (Roche). Nitroblue-tetrazolium-chloride/5-bromo-4-chloro-3-indolyl-phosphate (Promega) was used as a substrate for visualization. Immunohistochemistry was performed afterward as described above.

Image acquisition and statistical analyses. Fluorescence was detected using a Zeiss LSM 780. Images were acquired with the 20× and 63× objective and colocalization was confirmed by 3-D reconstructions of *z* series. Cell counts were performed using every sixth section throughout the rostrocaudal extent of the granule cell layer (GCL) and expressed as a percentage of double-labeled cells. DCX^+ retrovirus-labeled cells were three-dimensionally reconstructed using the Neurolucida software (MBF Bioscience) at 2 weeks postinjection (WPI) and 6 WPI (for FZD3 mutants). Individual neuron traces (between 45 and 80 for each group and time point) were analyzed with appropriate plug-ins of the Neurolucida Explorer (MBF Bioscience) and the CircStat toolbox for MATLAB (MathWorks). Sholl plots were compiled from the 3-D vector-based Neurolucida datasets by using 10 μm increment concentric circles around the center of the soma. All numerical analyses were performed using Excel (Microsoft) and GraphPad Prism. The unpaired Student's *t* test was used to compare averages between two groups. Comparisons between three or more groups were performed using a one-way ANOVA, followed by a Bonferroni *post hoc* test. The Kolmogorov–Smirnov (K–S) test was used to compare cumulative distributions (dendritic initiation sites, dendritic length).

Western blotting and qRT-PCR. Total RNA was extracted using RNA-Bee (Tel-Test) reagent and reversely transcribed into cDNA using the SuperscriptIII Kit (Invitrogen). Quantitative RT-PCR was performed using the C1000 Touch cycler (Bio-Rad) with the following primers: rat *β-actin*: 5′-AGGCCAACCGTGAAAAGATG-3′ and 5′-CCAGAGGCATACAGGGACAAC-3′; rat *Atp6ap2*: 5′-TGGGAAGCGTTATGGAGAAG-3′ and 5′-CTTCCTCACCAGGGATGTGT-3′; rat *Celsr1*: 5′-ACCTACCTGAGGCCCTTCAT-3′ and 5′-TGAACGTCCTGGAACCTTGG-3′; rat *Celsr2*: 5′-GAGCGAGGAAATGAACTCAGCC-3′ and 5′-TGAGCACTGGGCTGTCACAC-3′; rat *Celsr3*: 5′-CTGGTGTGCAAACAAGCTCC-3′ and 5′-GATGAAGTCCTTGCGGGACA-3′; rat *Fzd3*: 5′-CACATTCCGTGTCCGTACCA-3′ and 5′-AAAGCTGGCCCATTCAAAGC-3′; rat *Fzd4*: 5′-CAACTTTCACGCCGCTCATC-3′

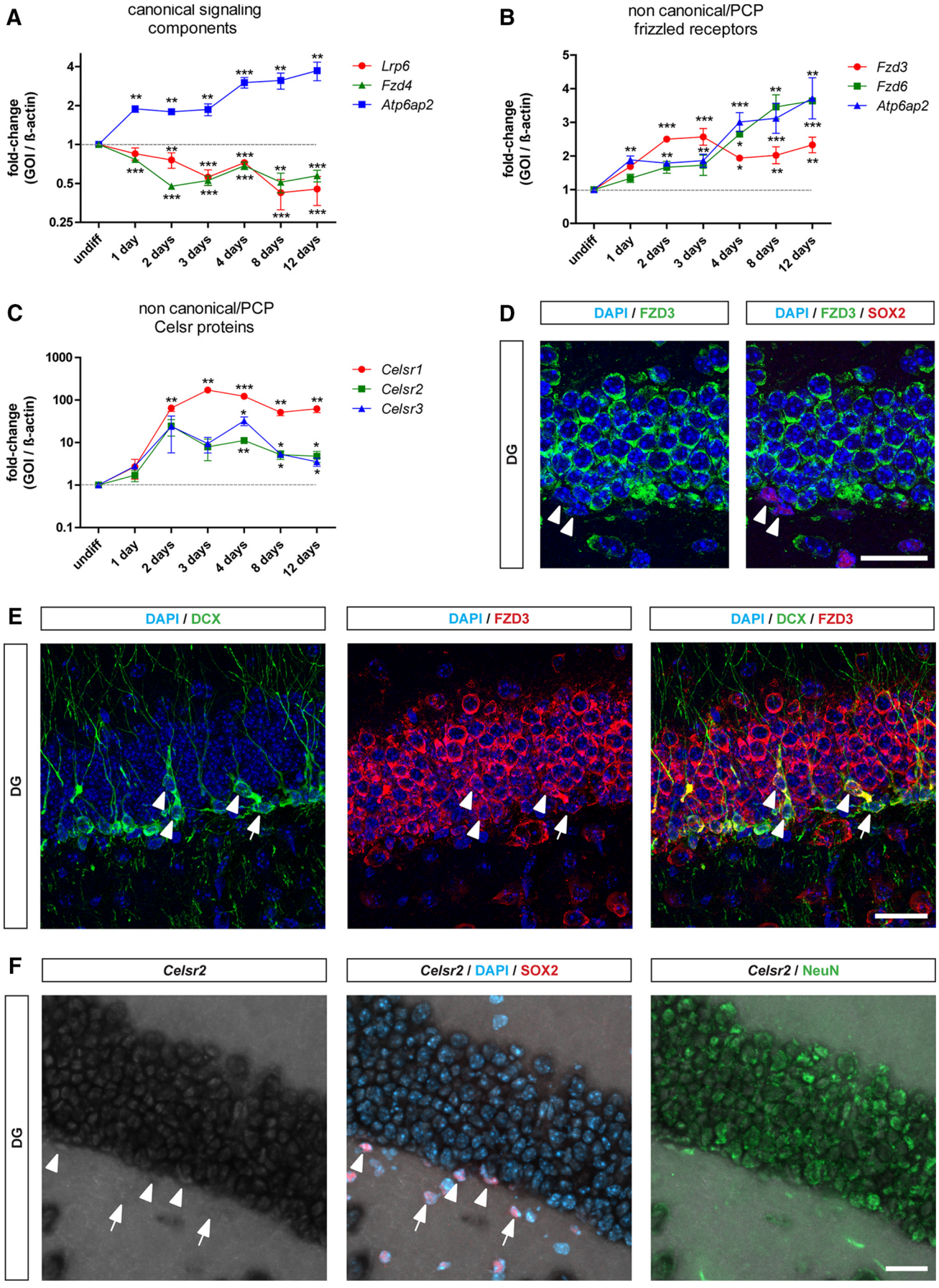
A
canonical signaling components
fold-change (GOI / ß-actin)
Lrp6
Fzd4
Atp6ap2
undiff
1 day
2 days
3 days
4 days
8 days
12 days
B
non canonical/PCP frizzled receptors
fold-change (GOI / ß-actin)
Fzd3
Fzd6
Atp6ap2
C
non canonical/PCP Celsr proteins
fold-change (GOI / ß-actin)
Celsr1
Celsr2
Celsr3
D
DAPI / FZD3
DAPI / FZD3 / SOX2
DG
E
DAPI / DCX
DAPI / FZD3
DAPI / DCX / FZD3
DG
F
Celsr2
Celsr2 / DAPI / SOX2
Celsr2 / NeuN
DG

and 5′-CTGAAAGACACATGCCACCG-3′; rat *Fzd6*: 5′-CCGATCGACGCCAGAGACAG-3′ and 5′-GCCGTTTCCTGAAAATGAGTTCT-3′; rat *Lrp6*: 5′-CTGAGTAAGCCCGTCGCTTT-3′ and 5′-CAGACCCACAGGCTGCAATA-3′; mouse *β-actin*: 5′-GGCTGTATTCCCCTCCATCG-3′ and 5′-CCAGTTGGTAACAATGCCATGT-3′; mouse *Atp6ap2*: 5′-ACCGGCCACGGGCTACCATTAT-3′ and 5′-TCGCTGGGAGCCAACTGCAA-3′; mouse *Celsr1*: 5′-TCCCAGCTCATCTTCATGGT-3′ and 5′-TGCAAGTTCTCCACAAGGGT-3′; mouse *Celsr2*: 5′-CCGAGAGGGTGGCTATACCT-3′ and 5′-GACACCTGGAGTACAACGGC-3′; mouse *Celsr3*: 5′-TTTGGTGTTTTGGCCACAGT-3′ and 5′-GAAGGCAGGGGAGGTACAGT-3′; mouse *Fzd3*: 5′-AAGACATGCTTTGAATGGGC-3′ and 5′-GGTCCCTCAGGAGTGACTGA-3′. Gene expression was normalized to β-actin and the relative gene expression was calculated using the ΔΔ*ct* method (Yuan et al., 2006).

Western blotting was performed as described previously (Schäfer et al., 2013). Briefly, proteins were separated by 4–12% PAGE, transferred to a nitrocellulose membrane, blocked and incubated with primary antibodies overnight at 4°C. The following antibodies were used: rabbit α-ATP6AP2 (1:500; Sigma-Aldrich), mouse α-β-actin (1:20.000; Sigma-Aldrich). To determine the activation of PCP downstream targets, undifferentiated and differentiated (2 d) AHPs were treated with 100 ng/ml WNT5A (R&D Systems) in the absence of differentiating factors for the time points indicated. Cells were lysed using a lysis buffer for phosphoproteins (50 mM β-glycerophosphate, pH 7.3, 1.5 mM EGTA, 1.0 mM EDTA, 0.1 mM sodium vanadate, 1.0 mM benzamidine, 10 μg/ml aprotinin, 10 μg/ml leupeptin, 2.0 μg/ml pepstatin A, 1.0 mM DTT) and subsequently centrifuged at 14,000 rpm at 4°C for 20 min. The procedure was performed as described above using the following primary antibodies: rabbit α-c-JUN (1:2000; Santa Cruz Biotechnology), rabbit α-phospho-c-Jun (1:500; Santa Cruz Biotechnology), rabbit α-SAPK/JNK (1:1000, Cell Signaling Technology), and rabbit α-phospho-SAPK/JNK (1:500; Santa Cruz Biotechnology). After extensive washes, membranes were incubated 1:10,000 with HRP-conjugated secondary antibodies (Jackson ImmunoResearch) for 2 h at room temperature. Antibody complexes were detected using an enhanced chemiluminescence reagent (Millipore) and quantified densitometrically.

Complex immunoprecipitation. Complex immunoprecipitations (Co-IPs) were performed using HEK293T or differentiated mouse Neuro2A cells (ATCC). Briefly, cells were transiently transfected with ATP6AP2-FLAG or CRF-FLAG in combination with CELSR2-HA or CELSR3-HA (a gift from Dr Uemura, Kyoto University, Japan). Cells were harvested, washed with PBS and lysed as described above in buffer containing 20 mM Tris, pH7.5, 150 mM NaCl, 2 mM $MgCl_2$, 1% Triton X-100, 1 mM DTT, and protease inhibitors (Roche). Following centrifugation, cell lysates containing equal amounts of protein were precleared at 4°C using A/G agarose beads (Santa Cruz Biotechnology) for 1 h. After preclearing, the lysates were incubated at 4°C overnight with α-FLAG bound agarose beads (Sigma-Aldrich). Beads were washed extensively with lysis buffer and bound proteins were resolved by SDS-PAGE using the following antibodies: rabbit α-FLAG (1:3000, Sigma-Aldrich), mouse α-FLAG (1:3000, Sigma-Aldrich), rat α-HA HRP (1:4000, Roche), and rabbit α-ATP6AP2 (1:500, Sigma-Aldrich). Secondary HRP-conjugated antibodies used included α-rabbit and α-mouse (1:5000; Jackson ImmunoResearch).

Results

During differentiation of AHPs, canonical Wnt signaling is attenuated whereas Wnt/PCP signaling is markedly upregulated

Previous studies have shown that canonical Wnt signaling is a principal regulator of adult hippocampal neurogenesis (Lie et al., 2005). Wnts are part of a complex and diverse set of pathways with a wide range of possible interactions. To examine the temporal activity of Wnt/β-catenin and Wnt/PCP signaling, we differentiated AHPs *in vitro* and quantified the levels of gene expression of several pathway components using quantitative real-time PCR (qRT-PCR). Upon differentiation, expression levels of canonical components such as *Lrp6* and *Fzd4* were gradually downregulated over the first 2–3 d and then remained low, whereas *Atp6ap2* expression became upregulated (Fig. 1*A*). Simultaneously, expression levels of *Fzd3* and *Fzd6* (Fig. 1*B*), as major Wnt/PCP receptors, and mRNA levels of core PCP genes *Celsr1-3* were continuously upregulated (Fig. 1*C*). Consistent with its up-regulation during *in vitro* differentiation, FZD3 appeared to be absent in $SOX2^+$ cells within the SGZ (Fig. 1*D*) but showed increasing abundance in cells of the neuronal lineage depending on their maturational stage (Fig. 1*E*). By combining *in situ* hybridization against *Celsr2* with immunohistochemistry-based fate mapping experiments, we were able to show that *Celsr2* expression is restricted to cells of the neuronal lineage (Fig. 1*F*). The same expression pattern was true for *Celsr1* and *Celsr3* (data not shown).

To characterize functional Wnt/β-catenin and Wnt/PCP signaling in differentiating AHPs, we performed luciferase reporter assays and compared their signaling response levels to undifferentiated control cells. AHPs were electroporated with TCF/LEF or AP-1 signaling reporters and subsequently cultured in the presence or absence of differentiating factors. WNT3A-induced TCF/LEF signaling was progressively attenuated during AHP differentiation, with a significant reduction of 58% after 2 d and 88% after 3 d of differentiation (Fig. 2*A*). In contrast, AP-1 activity significantly increased after 2 and 4 d of differentiation, with a 2.7- and 11-fold increase in reporter activity, respectively (Fig. 2*B*).

To test whether Wnt/PCP signaling responded to non-canonical ligands, such as WNT5A, in a stage-specific manner, we performed AP-1 reporter assays in differentiating and proliferating AHPs. Consistently, non-canonical WNT5A activated AP-1 signaling in differentiating AHPs but not in undifferentiated progenitors (Fig. 2*C*). Canonical pathway activators, such as WNT3A and the GSK-3β inhibitor CHIR, were unable to activate AP-1 signaling under either condition (Fig. 2*C*). WNT5A has been shown to activate PCP signaling, which leads to the subsequent phosphorylation of JNK and its downstream target c-Jun (Yamanaka et al., 2002; Wang et al., 2013). To determine their stage-specific level of activation, we performed semiquantitative Western blot analyses of c-JUN phosphorylation in proliferating and differentiating AHPs. In proliferating AHPs, acute stimulation with WNT5A did not induce phosphorylation of PCP downstream target c-JUN (Fig. 2*D*), whereas in differentiating AHPs a significant WNT5A-induced phosphorylation of c-JUN appeared 15 min after ligand application (Fig. 2*E*,*F*).

Furthermore, knockdown of FZD3 in differentiating AHPs was sufficient to reduce the WNT5A-induced phosphorylation of both JNK and c-JUN (Fig. 2*G*,*H*). These data suggest that FZD3 acts upstream of JNK and c-JUN and that shRNA-mediated si-

←

Figure 1. Temporal expression patterns of Wnt/β-catenin and Wnt/PCP pathway components during dentate granule cell differentiation. ***A***, *Lrp6* and *Fzd4* mRNA levels are gradually decreased in differentiating AHPs relative to undifferentiated control cells as measured by qRT-PCR, whereas *Atp6ap2* expression becomes upregulated. ***B***, ***C***, Expression levels of *FZD3* and *FZD6*, as well as *Celsr1-3* are progressively upregulated upon differentiation of AHPs, similar to the levels of *Atp6ap2*. ***D***, FZD3 (green) is not expressed by $SOX2^+$ cells (red) in the SGZ (arrowheads). DAPI (blue), FZD3 (green), SOX2 (red). Scale bar 25 μm. ***E***, DCX^+ cells (green) show increasing abundance of FZD3 (red), including immature DCX^+ cells in the SGZ (arrows) as well as DCX^+ cells that extended their dendrites toward the molecular layer (arrowheads). DAPI (blue), DCX (green), and FZD3 (red). Scale bar, 25 μm. ***F***, Combined *in situ* hybridization against *Celsr2* mRNA (gray) with immunostaining against SOX2 (red) and NeuN (green). The specificity of the signal was confirmed by using the *Celsr2* sense-probe as control (data not shown). *Celsr2* mRNA is not expressed by $SOX2^+$ cells (red) in the SGZ (arrowheads) and the hilus (arrows). $NeuN^+$ cells (green) show high-level expression of *Celsr2* mRNA. DAPI (blue), NeuN (green), SOX2 (red), and *Celsr2* mRNA (gray). Scale bar, 25 μm. Results are expressed as mean ± SEM ($n \geq 5$ per group); $^*p < 0.05$, $^{**}p < 0.01$, $^{***}p < 0.001$.

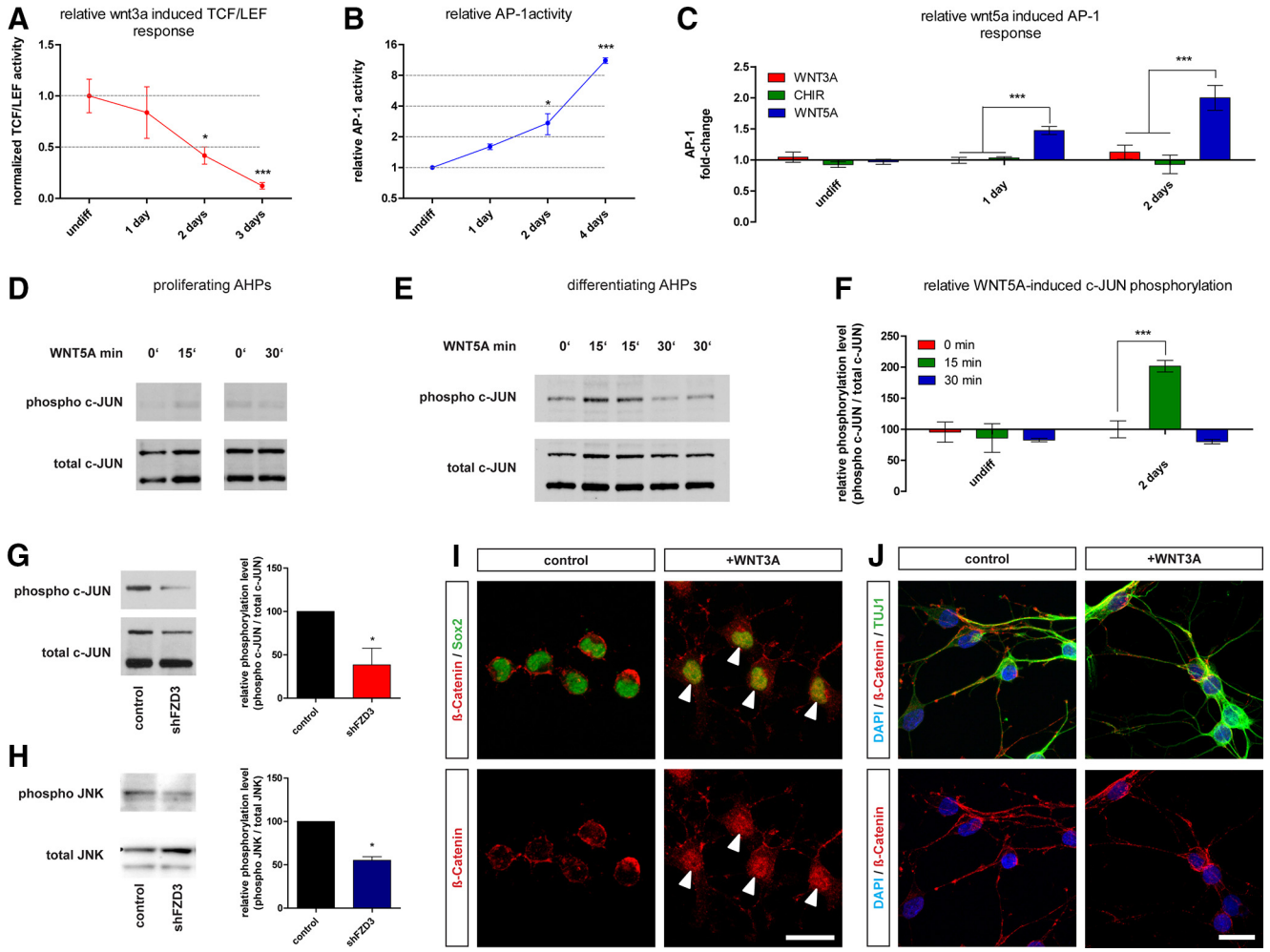

Figure 2. Wnt/β-catenin pathway is attenuated whereas Wnt/PCP pathway is upregulated upon differentiation of AHPs *in vitro*. ***A***, WNT3A-induced TCF/LEF response is significantly attenuated in AHPs 2 d ($p < 0.05$) and 3 d ($p < 0.001$) after differentiation. ***B***, AP-1 signaling response is markedly increased after 2 d ($p < 0.05$) and 3 d ($p < 0.001$) in differentiating conditions. ***C***, WNT5A activated non-canonical AP-1 signaling only in AHP-derived neuroblasts but failed to do so in undifferentiated AHPs. Canonical pathway activators WNT3A and CHIR were unable to induce a non-canonical AP-1 signaling response (1 and 2 d of differentiation). ***D***, In proliferating AHPs, acute stimulation with WNT5A did not induce phosphorylation of PCP downstream target c-JUN (Ser63) either 15 min or 30 min after ligand application. ***E***, In differentiating AHPs (2 d), a significant WNT5A-induced phosphorylation of c-JUN (Ser63) appeared 15 min after ligand application. ***F***, Relative phosphorylation levels of c-JUN after stimulation with WNT5A for the time points indicated. Total c-JUN protein levels were used to normalize the phosphorylation signal. ***G***, Representative images of WNT5A-induced phosphorylation of c-JUN (Ser63) in 2-d-old neuroblasts. FZD3-deficient cells showed significantly reduced phosphorylation levels of c-JUN after 15 min of ligand application compared with controls. Total c-JUN protein levels were used to normalize the phosphorylation signal. ***H***, Representative images of WNT5A-induced phosphorylation of JNK (Thr183/Tyr185) in 2-d-old neuroblasts. FZD3-deficient cells showed significantly reduced phosphorylation levels of JNK after 15 min of ligand application compared with controls. Total JNK protein levels were used to normalize the phosphorylation signal. ***I***, Localization of β-catenin in untreated (control) and WNT3A-treated undifferentiated AHPs (arrowheads). SOX2 (green), β-catenin (red). Scale bar, 20 μm. ***J***, Localization of β-catenin in untreated (control) and WNT3A-treated differentiating AHPs. DAPI (blue), TUJ1 (green), and β-catenin (red). Scale bar, 20 μm. Results are expressed as mean ± SEM ($n \geq 5$ per group); $^{*}p < 0.05$, $^{**}p < 0.01$, $^{***}p < 0.001$.

lencing of FZD3 is sufficient to attenuate the WNT5A-induced activation of those kinases in differentiating neuroblasts.

To confirm our findings regarding the maturational attenuation of canonical Wnt signaling, we performed an *in vitro* β-catenin translocation assay in AHPs. Consistent with the signaling reporter assays, WNT3A-induced β-catenin translocation into the nucleus only appeared in undifferentiated AHPs but not in differentiated AHPs (Fig. 2*I*,*J*).

Dual role of ATP6AP2 in both canonical Wnt signaling in proliferating AHPs and non-canonical Wnt signaling in differentiating AHPs

The accessory subunit of the V-ATPase, ATP6AP2, was shown to function as both a Wnt/PCP core protein and an important adaptor protein to initiate canonical Wnt signaling (Buechling et al., 2010; Cruciat et al., 2010; Hermle et al., 2013). To clarify the possible dual role of ATP6AP2 in neurogenic Wnt signaling, we first analyzed the effect of ATP6AP2 knockdown on Wnt/β-catenin and Wnt/PCP signaling *in vitro* using shRNA (shATP6AP2 #1 and #2). Knockdown of ATP6AP2 in AHPs resulted in a significant reduction in WNT3A-induced TCF/LEF reporter activity (Fig. 3*A*). The same effect was also observed in cells that were not treated with WNT3A but instead were plated on hippocampal astrocytes to mimic the adult hippocampal niche *in vitro* (Fig. 3*B*; Song et al., 2002). Overexpression of the full-length protein in ATP6AP2-deficient cells was able to rescue the phenotype (Fig. 3*C*), whereas simultaneous overexpression of a truncated version of ATP6AP2 lacking the essential LRP6 binding domain (ΔECD-ATP6AP2) was not sufficient to rescue the reduced canonical signaling response in proliferating AHPs (Fig. 3*C*).

To test whether ATP6AP2 knockdown also affected Wnt/PCP signaling, we differentiated AHPs for 2 d and compared the

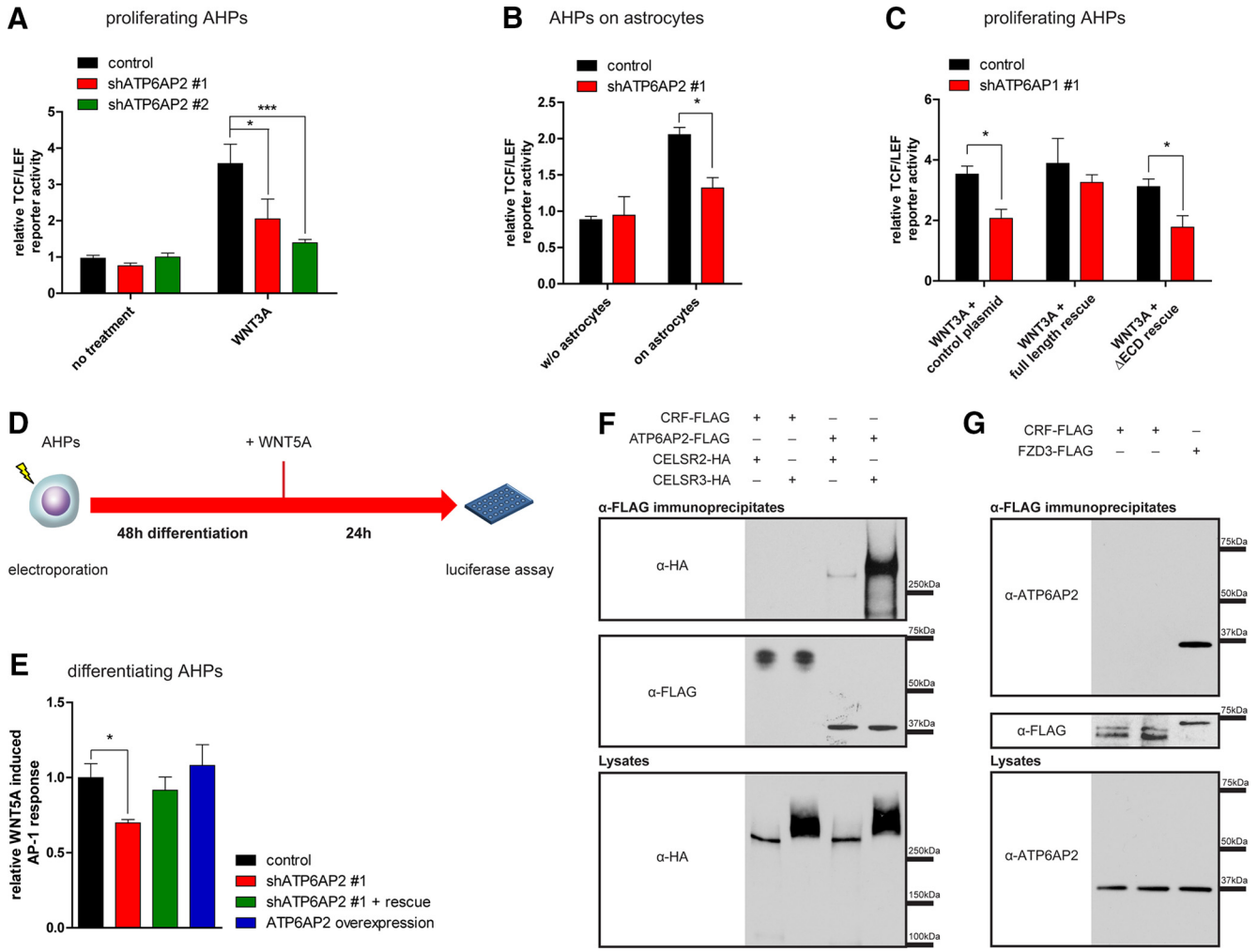

Figure 3. The adaptor protein ATP6AP2 is involved in Wnt/β-catenin and Wnt/PCP signaling of AHPs *in vitro*. ***A***, WNT3A-induced TCF/LEF reporter activity is notably reduced in proliferating AHPs expressing the weaker ATP6AP2 targeting shRNA (shATP6AP2 #1; $p < 0.05$). This reduction in WNT3A-induced TCF/LEF response is even more pronounced in cells expressing the stronger shRNA (shATP6AP2 #2; $p < 0.001$). ***B***, Knockdown of ATP6AP2 in AHPs plated on hippocampal astrocytes resulted in a significant reduction in TCF/LEF reporter activity as compared with control cells (shATP6AP2 #1; $p < 0.05$). ***C***, Overexpression of the full-length protein in ATP6AP2-deficient AHPs rescued the reduced canonical signaling response. Simultaneous overexpression of a truncated version of ATP6AP2 lacking the essential LRP6 binding domain (ΔECD-ATP6AP2) was not sufficient to rescue TCF/LEF signaling response in proliferating AHPs. ***D***, Experimental procedure of Wnt/PCP reporter assays. ***E***, In differentiating AHPs, the WNT5A-induced AP-1 signaling response was significantly reduced in those neuroblasts expressing shATP6AP2 ($p < 0.05$). Simultaneous overexpression of the full-length protein rescued the phenotype. Overexpression of ATP6AP2 alone was not sufficient to increase AP-1 reporter activity. ***F***, FLAG-tagged ATP6AP2 or the control transmembrane protein CRF was coexpressed with HA-tagged CELSR2 or CELSR3 in HEK293T cells. After immunoprecipitation with α-FLAG, CELSR2 and 3 bound to immunoprecipitated ATP6AP2 but not to the control protein CRF (3–8%, Tris-acetate SDS-PAGE). ***G***, In differentiated mouse Neuro2A cells, endogenous ATP6AP2 was present in immunoprecipitates formed by FZD3-FLAG but not in those formed by the control transmembrane protein CRF (4–12% Bis-Tris, MOPS SDS-PAGE). Results are expressed as mean ± SEM ($n \geq 4$ per group); *$p < 0.05$, **$p < 0.01$, ***$p < 0.001$.

WNT5A-induced AP-1 signaling response of ATP6AP-deficient cells with their respective control groups (Fig. 3*D*). Cells expressing shATP6AP2 #1 displayed significantly reduced AP-1 signaling in response to WNT5A, which was again rescued by overexpression of the full-length protein (Fig. 3*E*). Overexpression of ATP6AP2 was not sufficient to enhance the signaling response, supporting its role as an adaptor protein (Fig. 3*E*). To obtain biochemical proof for the interaction between ATP6AP2 and PCP components, we performed coimmunoprecipitation experiments. Transient transfection of HEK293T cells with murine versions of CELSR2 and 3, and ATP6AP2 resulted in sufficient protein expression levels. In these cells, we observed that immunoprecipitation of ATP6AP2 retained CELSR2 and CELSR3, whereas antibodies against the control transmembrane protein CRF did not (Fig. 3*F*). Furthermore, immunoprecipitation of FZD3 in differentiated mouse Neuro2A cells retained endogenous ATP6AP2, which was not observed when pulling down the control transmembrane protein CRF (Fig. 3*G*). Altogether, these data confirm the dual role for ATP6AP2 in Wnt signaling during neurogenesis and provide evidence of a physical interaction with the PCP complex.

Knockdown of ATP6AP2 affects both cell fate determination and morphogenesis of adult-born granule cells

Given the different expression patterns of Wnt pathway components and the transition of the specific Wnt signaling response in the course of AHP differentiation, we analyzed the functional role of ATP6AP2 in early and late steps of adult hippocampal neurogenesis *in vivo*. Because ATP6AP2 is involved in canonical Wnt and Wnt/PCP signaling, its effect on adult neurogenesis should depend on the respective pathway that is active at a particular stage. To address this question and to be able to titrate down the actual signal strength of Wnt/β-catenin signaling, we designed two retroviral (RV) vectors that encoded for GFP and expressed

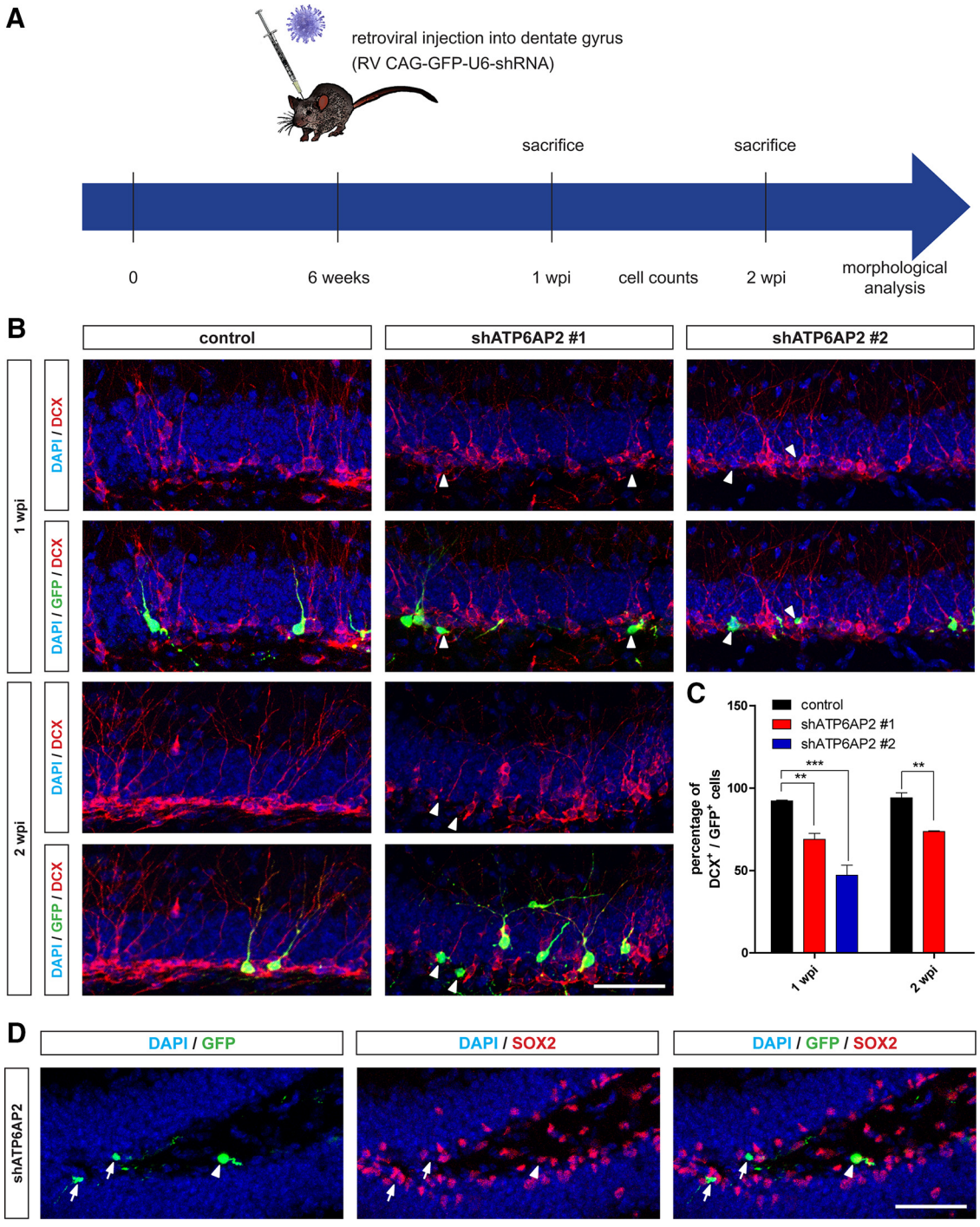

Figure 4. Knockdown of ATP6AP2 affects cell fate commitment of adult hippocampal stem cells. ***A***, A schematic diagram of the experimental design. Stereotactic injections were placed into the DG of 6- to 7-week-old mice using shRNA- and GFP-expressing retroviral vectors. Animals were killed either on 1 or 2 WPI and subjected to stereological and morphometric analyses. ***B***, ***C***, Adult-born neurons (shown in green) express the early neuronal marker DCX (shown in red) from 1 week after birth onward. A marked reduction in the number of GFP^+DCX^+ double-labeled newborn cells was seen in shATP6AP2 #1 ($p < 0.01$) and was even more pronounced in shATP6AP2 #2-expressing cells ($p < 0.001$) compared with animals injected with nontargeting shRNA-expressing control viruses (arrowheads show undifferentiated DCX^- cells). DAPI (blue), GFP (green), and DCX (red). ***D***, Among the population of GFP^+DCX^+ cells, some remained SOX2-positive (arrowheads), whereas some lost their SOX2 expression (arrows). GFP (green), DAPI (blue), and Sox2 (red). Error bars represent mean ± SEM ($n \geq 3$ mice per group); $^*p < 0.05$, $^{**}p < 0.01$, $^{***}p < 0.001$. Scale bars, 50 μm.

shRNAs that had a mild (shATP6AP2 #1) or strong (shATP6AP2 #2) knockdown efficiency. We then stereotactically injected these shRNA-expressing retroviruses into the DG of young adult mice (6–7 weeks old) to assess the effect of ATP6AP2 knockdown in dividing neural progenitor cells *in vivo* (Fig. 4*A*; Zhao et al., 2006).

Using doublecortin (DCX) staining as a measure to quantify neuronal differentiation, we found a marked reduction in the number of GFP^+DCX^+ double-labeled newborn neurons in shATP6AP2 mice compared with animals injected with nontargeting shRNA-expressing control viruses (Fig. 4*B*). In-line with a stronger effect of shATP6AP2 #2 on Wnt/β-catenin signaling *in*

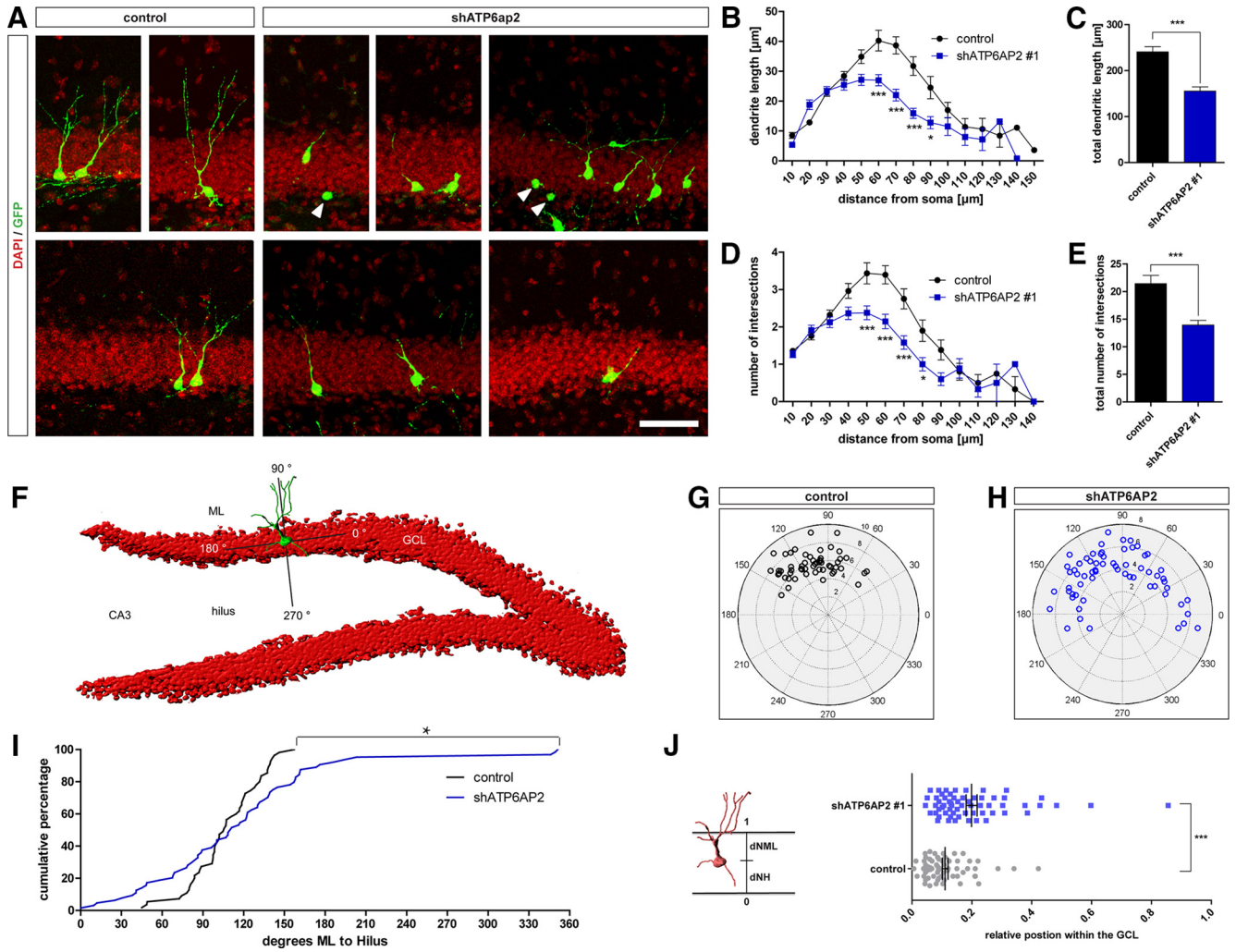

Figure 5. ATP6AP2-deficient DCX$^+$ cells display impaired morphological development. ***A***, Two-week-old ATP6AP2-deficient neurons (green) that express DCX are among those that remained undifferentiated (arrowheads). Only GFP$^+$DCX$^+$ cells were reconstructed for morphometric analyses. DAPI (red); GFP (green). ***B***, Sholl analysis of the dendritic length of GFP$^+$DCX$^+$ neurons. The data represent mean ± SEM (number of traced neurons: control: $n = 53$; shATP6AP2: $n = 56$; $^*p < 0.05$, $^{***}p < 0.001$, Student's t test). ***C***, Total dendritic length of GFP$^+$DCX$^+$ neurons ($^{***}p < 0.001$, Student's t test). ***D***, Sholl analysis of the dendritic complexity of GFP$^+$DCX$^+$ neurons (same groups of cells as in ***B*** were analyzed; $^*p < 0.05$, $^{***}p < 0.001$, Student's t test). ***E***, Total number of intersections of GFP$^+$DCX$^+$ neurons ($^{***}p < 0.001$, Student's t test). ***F***, A schematic model of analyses performed to quantitatively assess the angular orientation of the dendritic initiation sites. As a reference, a coordinate system was established with the x-axis parallel to the granule layer (0°–180°), the y-axis pointing toward the hilus or molecular layer (90° and 270°) and the origin at the center of the soma. ML, Molecular layer; CA3, cornu ammonis 3. ***G***, ***H***, Angular orientation of dendritic initiation sites of control (***G***) and ATP6AP2-deficient (***H***) GFP$^+$DCX$^+$ neurons within the GCL. ***I***, Cumulative distribution plots of initiation sites revealed a significant difference between control and ATP6AP2-deficient neurons ($^*p < 0.05$, K–S test). ***J***, Quantitative analyses of the migratory properties of newborn granule cells. Shown are the relative positions of GFP$^+$DCX$^+$ neurons within the GCL. The relative position of ATP6AP2-deficient neurons is significantly shifted toward the molecular layer compared with control cells ($^{***}p < 0.001$, Student's t test). dNML, Distance from neuronal soma to molecular layer; dNH, distance from neuronal soma to hilus.

vitro (Fig. 3), animals injected with shATP6AP2 #2 expressing retroviruses showed an even more pronounced reduction in the levels of neurogenesis (Fig. 4*C*). Among the population of undifferentiated GFP$^+$DCX$^-$ cells, no increase in caspase3-activity was detected (data not shown) and only a few of the cells colabeled with the stem cell marker SOX2 (Fig. 4*D*). Interestingly, GFP$^+$DCX$^+$ in both shATP6AP2 conditions displayed marked defects in several aspects of morphological development (Fig. 5*A*). We analyzed these defects using 3-D reconstructions of GFP$^+$DCX$^+$ neurons and assessed their morphology. At 2 WPI, we found that ATP6AP2-deficient GFP$^+$DCX$^+$ neurons had significantly shorter dendrites and reduced dendritic arborization compared with control cells (Fig. 5*B–E*). Further examination of individual GFP$^+$DCX$^+$ neurons revealed that the initiation sites of most primary dendrites in control cells were oriented toward the molecular layer, whereas many ATP6AP2-deficient neurons pointed parallel to the granule layer. Quantitative analyses were performed by defining the angular orientation of the initiation site on the soma (Shelly et al., 2010), with the x-axis parallel to the granule layer (0°–180°), the y-axis pointing toward the hilus or molecular layer (90° and 270°) and the origin at the center of the soma (Fig. 5*F*). Normal newborn neurons initiated their dendrites preferentially within ~45°–150° toward the molecular layer (Fig. 5*G*). However, analyses of ATP6AP2-deficient cells indicated a random distribution of initiation sites within ~350°–210°, excluding the hilus (Fig. 5*H*). Cumulative distribution plots of initiation sites showed a significant difference between control and ATP6AP2-deficient neurons (Fig. 5*I*; $p < 0.05$, K–S test). Regarding their position within the DG, control cells remained within the first third of the granular layer, in close proximity to the SGZ, and only a few cells migrated further. In contrast, the relative position of ATP6AP2-deficient neurons was significantly shifted toward the molecular layer (Fig. 5*J*), suggesting an involvement in regulating the migration of newborn neurons. To

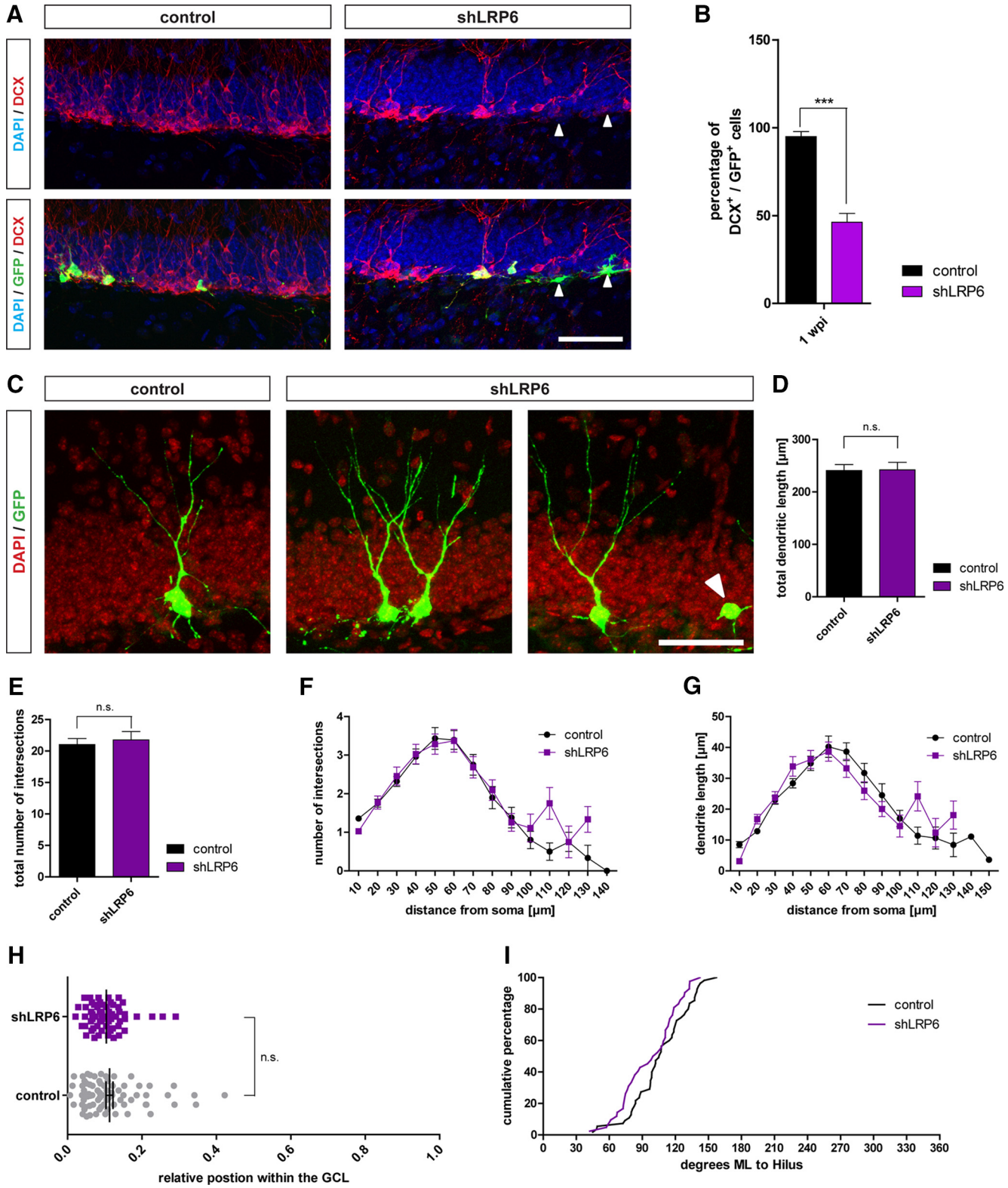

Figure 6. LRP6 is critically involved in granule cell fate commitment but not morphogenesis. ***A***, ***B***, The early neuronal marker DCX (shown in red) is expressed by adult-born neurons (shown in green) 1 week after birth. A marked reduction in the number of GFP $^{+}$DCX $^{+}$ double-labeled newborn cells was seen in shLRP6-expressing cells ($p < 0.001$) compared with animals injected with nontargeting shRNA-expressing control viruses (arrowheads show undifferentiated DCX $^{-}$ cells). DAPI (blue), GFP (green), and DCX (red). Scale bar, 50 μm. ***C***, Representative images of 2-week-old GFP $^{+}$DCX $^{+}$ cells. Undifferentiated DCX $^{-}$ cells (arrowheads). GFP (green); DAPI (red). Scale bar, 50 μm. ***D***, Total dendritic length of GFP $^{+}$DCX $^{+}$ neurons. The data represent mean ± SEM (number of traced neurons: control: $n = 53$; shLRP63: $n = 35$ (n.s., Student's t test). ***E***, Total number of intersections of GFP $^{+}$DCX $^{+}$ neurons (same groups of cells as in ***D*** were analyzed; n.s., Student's t test). ***F***, Sholl analysis of the dendritic length of GFP $^{+}$DCX $^{+}$ neurons. The data represent mean ± SEM (same groups of cells as in ***D*** were analyzed; n.s., Student's t test). ***G***, Sholl analysis of the dendritic complexity of GFP $^{+}$DCX $^{+}$ neurons (same groups of cells as in ***D*** were analyzed; n.s., Student's t test). ***H***, Relative positions of GFP $^{+}$DCX $^{+}$ neurons within the GCL. The relative position within the GCL of LRP6-deficient neurons is statistically not different from the respective control group (n.s., Student's t test). ***I***, Cumulative distribution plots of the angular orientation of dendritic initiation sites. (n.s., K–S test). Results are expressed as mean ± SEM ($n \geq 4$ animals per group); *$p < 0.05$, **$p < 0.01$, ***$p < 0.001$, n.s., not significant; $p > 0.05$.

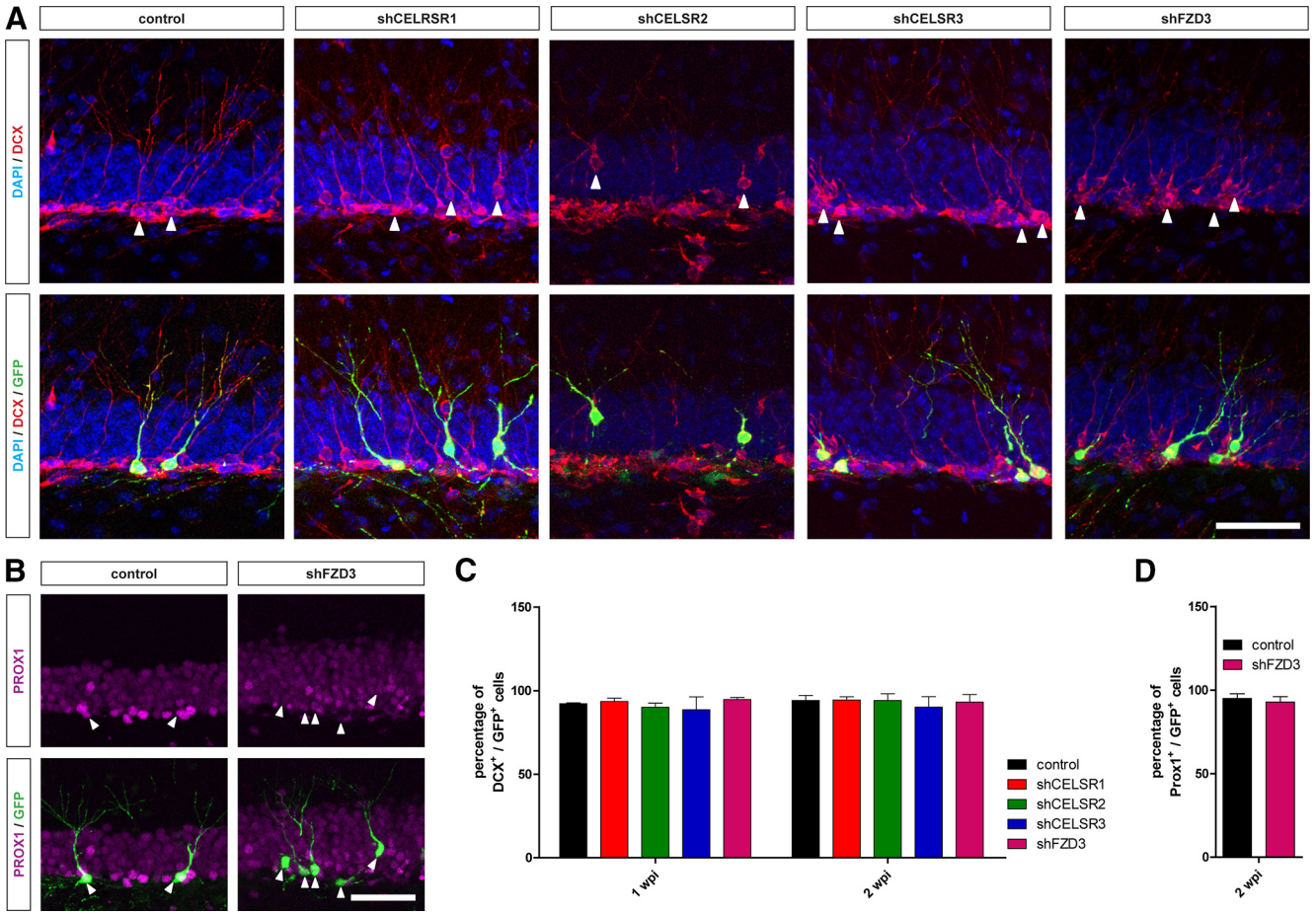

Figure 7. Knockdown of PCP core proteins does not affect cell fate determination of adult hippocampal stem cells. ***A***, Representative images of 2-week-old PCP mutants shFZD3 and shCELSR1-3, as well as control cells (green) that were committed to a neuronal cell fate (arrowheads). GFP (green), DCX (red), and DAPI (blue). Scale bar, 50 μm. ***B***, Two-week-old FZD3 mutants express the granule cell marker PROX1 (magenta; arrowheads). Scale bar, 50 μm. ***C***, Quantitative analyses of GFP$^+$DCX$^+$ cells in the DG 1 and 2 WPI expressed as a percentage of the total number of GFP$^+$ cells. The data represent mean ± SEM ($n \geq 3$ animals per group). ***D***, Quantification of GFP$^+$PROX1$^+$ double-labeled cells 2 WPI expressed as a percentage of the total number of GFP$^+$ cells. The data represent mean ± SEM ($n \geq 3$ animals per group).

compare these phenotypes with canonical signaling mutants, we took advantage of retrovirus-based silencing of the canonical coreceptor LRP6. We found that LRP6-deficient animals had reduced levels of neurogenesis as measured by DCX staining (Fig. 6*A*,*B*), but among the population of GFP$^+$DCX$^+$ cells expressing shLRP6 morphological development appeared to be unaffected (Fig. 6*C*–*I*). Together, reduced levels of ATP6AP2 in neural progenitor cells resulted in a decreased induction of neuronal cell fate similar to what was seen in LRP6 mutants but also caused severe morphological defects in newborn neurons. Thus, defects in cell fate and morphogenesis in ATP6AP2-defcient cells is likely to be the consequence of altering both canonical and non-canonical Wnt signaling.

PCP core proteins are not critically involved in cell-fate determination but control several aspects of morphological development

We next asked which components of Wnt/PCP signaling were possible candidates accounting for the morphological impairments seen in ATP6AP2-deficient newborn neurons. *Celsr1-3*, the mammalian orthologs of *flamingo*, and *Fzd3* are among the core PCP genes and are widely expressed in the nervous system (Feng et al., 2012a). FZD3 and CELSR1-3 have been described to be involved in many aspects of morphogenesis (Tissir and Goffinet, 2013), and thus represent attractive candidates that might be instrumental in the morphological specification of newborn granule cells. To characterize whether Wnt/PCP signaling had a stage-specific function in the course of adult hippocampal neurogenesis, we used a retrovirus-based approach to deliver shRNAs specifically targeting PCP core proteins CELSR1-3 and FZD3. We first analyzed the quantity of neurogenesis by using DCX staining and found no differences in the number of newborn DCX$^+$ cells between PCP mutants shFZD3, shCELSR1-3, and control animals (Fig. 7*A*,*B*). Likewise, at 2 WPI, almost every FZD3-deficient cell expressed the granule cell marker PROX1 as in the control group (Fig. 7*C*,*D*) and 6 WPI PCP mutants expressed mature neuron marker Calbindin (data not shown). These results illustrate that Wnt/PCP signaling does not appear to be critically involved in cell-fate determination during adult neurogenesis.

Given the importance of FZD3 in PCP signaling and the observation that this pathway does not affect cell fate commitment, we first focused on the role of FZD3 in later stages of adult hippocampal neurogenesis. Therefore, we assessed morphological features such as dendritic growth, migratory behavior, and cell orientation of FZD3-deficient cells *in vivo*. As seen with ATP6AP2-deficient neurons, shFZD3-expressing cells abnormally migrated toward the molecular layer (Fig. 8*B*). Morphological assessment of FZD3-deficient cells demonstrated that newborn DCX$^+$ cells had significantly shorter dendrites and a

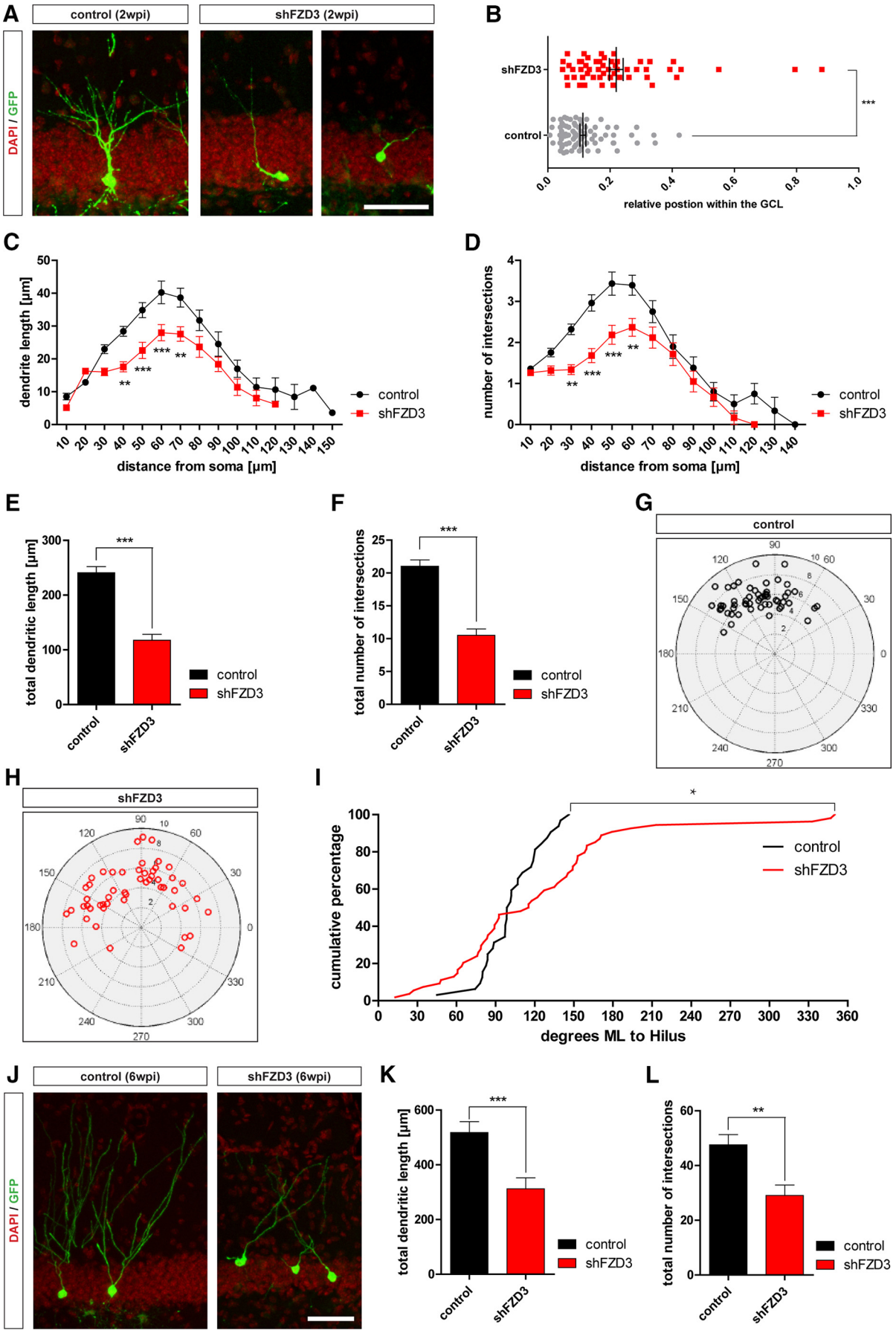
A
control (2wpi)
shFZD3 (2wpi)
DAPI / GFP
B
shFZD3
control
***
0.0
0.2
0.4
0.6
0.8
1.0
relative postion within the GCL
C
dendrite length [µm]
distance from soma [µm]
control
shFZD3
D
number of intersections
distance from soma [µm]
control
shFZD3
E
total dendritic length [µm]
control
shFZD3
F
total number of intersections
control
shFZD3
G
control
H
shFZD3
I
cumulative percentage
degrees ML to Hilus
control
shFZD3
J
control (6wpi)
shFZD3 (6wpi)
DAPI / GFP
K
total dendritic length [µm]
control
shFZD3
L
total number of intersections
control
shFZD3

reduced dendritic arborization compared with control cells expressing a nontargeting shRNA (Fig. 8*C–F*). Furthermore, the orientation of dendrite initiation sites of shFZD3-expressing cells appeared to be randomly distributed within ~330° and 213° (Fig. 8*G–I*). As with shATP6AP2-expressing cells, the orientation of their dendrite initiation sites excluded the hilus. A K–S test comparing both groups revealed a significant difference between control and FZD3-deficient neurons ($p < 0.05$, K–S test). Defects in dendritic growth of FZD3-deficient neurons were present even 6 WPI (Fig. 8*J–L*). These data showed that knockdown of FZD3 resembled all assessed phenotypic features of ATP6AP2-deficient cells that were committed to a neuronal cell fate, confirming a pivotal role for FZD3-mediated Wnt/PCP signaling at these morphogenic stages.

CELSR1-3 control distinctive aspects of PCP-mediated granule cell morphogenesis

As FZD3 controls several morphological aspects of developing cells, and CELSR1, 2, and 3 represent core proteins involved in the same signaling pathway, we next asked whether they control the same morphogenic features. CELSRs cooperatively interact with PCP members during development (Feng et al., 2012a) and might therefore control distinctive morphogenic aspects during the development of newborn neurons. To address this possibility, we sought to dissect out the individual roles of CELSR1, CELSR2, and CELSR3 by performing a differential phenotype screen among these PCP mutants. Sholl-analyses of PCP mutants revealed that both CELSR2- and CELSR3-deficient neurons showed a significant reduction in dendritic length and a less complex arborization compared with control cells. In contrast, no differences in dendritic growth were seen in shCELSR1-expressing cells (Fig. 9*A–C*). However, only shCELSR1-expressing cells displayed a random distribution of initiation sites, whereas shCELSR2- and shCELSR3-expressing cells preferentially initiated their dendrites toward the molecular layer. Cumulative distribution plots revealed a significant difference between control and CELSR1-deficient neurons ($p < 0.05$, K–S test), similar to what was seen with FZD3-deficient cells (Fig. 9*D*). Furthermore, migratory defects were found in CELSR2- and CELSR3-deficient neurons but not in those expressing shCELSR1 (Fig. 9*E*), suggesting that CELSR2 and 3 control migration and dendritic outgrowth directly at the growth cone. Furthermore, HA-tagged CELSR2 and 3 localize in proximity to the cell membrane of extending neurites in differentiating AHPs and are even more enriched in filopodia-like structures, emphasizing their direct localized involvement in dendritic morphogenesis (Fig. 9*F*).

Overall, our results demonstrate distinct roles for CELSR1, 2, and 3 in newborn granule cell morphogenesis that are all cooperatively represented in FZD3-deficient cells.

Discussion

NSCs in the adult hippocampus preserve a regenerative capacity throughout adulthood. Within the adult brain, only the SVZ and the DG produce substantial numbers of new neurons throughout life. Therefore, these two niches are thought to provide all necessary cues to support the neurogenic potential of adult NSCs. WNT3 is one of the key molecules expressed by local astrocytes within the SGZ of the DG, acting as a principal regulator of adult NSC differentiation (Lie et al., 2005; Jessberger et al., 2009; Kuwabara et al., 2009; Karalay et al., 2011). Wnts comprise a large family of secreted glycoproteins (van Amerongen and Nusse, 2009) and form part of a diverse set of different pathways. Because all steps of adult hippocampal neurogenesis occur in the SGZ of the DG in close proximity, factors regulating distinctive steps should be constantly present. A stage-specific function of different Wnt pathways could then only be realized through the expression of distinctive Wnt receptor combinations.

We found that *Fzd4* and the canonical coreceptor *Lrp6* are downregulated, whereas Wnt/PCP components *Fzd3*, *Fzd6*, and *Celsr1-3* are markedly upregulated upon differentiation of AHPs. Canonical Wnt/β-catenin signaling is highly LRP6-dependent and FZD4 has been shown to be an important receptor for TCF/LEF signaling. However, in some cases, non-canonical Wnts such as WNT5A are able to activate the canonical signaling cascade through FZD4 only in combination with LRP6 (Ring et al., 2014). In this scenario, a downregulation of both signaling components might be a prerequisite to inactivate canonical signaling cascades even in the presence of Wnt ligands. Consistently, upon differentiation the actual WNT3A-induced canonical TCF/LEF response was attenuated and non-canonical Wnt/PCP AP-1 signaling responses continuously increased. In-line with this finding, a loss of *LEF1* expression during the differentiation of dentate progenitors has been reported in the developing hippocampus (Galceran et al., 2000), and reporter mice revealed a downregulation of Wnt/β-catenin signaling at the neuroblast stage (Garbe and Ring, 2012). These observations are consistent with our findings that WNT3A-induced β-catenin translocation into the nucleus only appears in undifferentiated adult NSCs.

Previous studies have shown that WNT3A and WNT5A have different roles in the development of olfactory bulb interneurons (Pino et al., 2011). Interestingly, WNT5A was able to activate a non-canonical signaling response only in differentiating neuroblasts but failed to do so when applied to undifferentiated AHPs. These stage-specific differences might be attributable to a highly context-specific response to Wnts during neurogenesis.

We further found that knockdown of ATP6AP2, an adaptor protein involved in both pathways (Buechling et al., 2010; Cruciat et al., 2010; Hermle et al., 2013), affected both cell fate determination and morphological maturation of adult-born granule cells. We tested whether ATP6AP2 knockdown affected Wnt signaling in adult NSCs and confirmed its dual role as an adaptor protein *in vitro*. In-line with this finding, Co-IP experiments revealed a specific interaction of ATP6AP2 with members of the PCP core family such as CELSR2 and 3, as well as FZD3. By using retroviruses expressing two shRNAs of different ATP6AP2 targeting strength, we were able to titrate down the actual signal strength of Wnt/β-catenin signaling *in vivo*. Newborn cells expressing shATP6AP2 showed a reduced ability to commit to a neuronal cell fate. Among RV-labeled cells that expressed the

←

Figure 8. FZD3 single-cell knockdown affects several aspects of granule cell morphogenesis. ***A***, Representative images of 2-week-old GFP$^+$DCX$^+$ cells. GFP (green); DAPI (red). Scale bar, 50 μm. ***B***, Quantification of the relative positions of 2-week-old GFP$^+$DCX$^+$ neurons within the GCL. FZD3-deficient neurons abnormally migrated further toward the molecular layer than control cells (***$p < 0.001$, Student's *t* test). ***C***, Sholl analysis of the dendritic length of 2-week-old GFP$^+$DCX$^+$ neurons. The data represent mean ± SEM (number of traced neurons: control: $n = 53$; shFZD3: $n = 61$; ***$p < 0.001$, Student's *t* test). ***D***, Sholl analysis of the dendritic complexity of 2-week-old GFP$^+$DCX$^+$ neurons (same groups of cells as in ***C*** were analyzed); *$p < 0.05$, **$p < 0.01$, Student's *t* test). ***E***, Total dendritic length of 2-week-old GFP$^+$DCX$^+$ neurons (***$p < 0.001$, Student's *t* test). ***F***, Total number of intersections of 2-week-old GFP$^+$DCX$^+$ neurons (***$p < 0.001$, Student's *t* test). ***G***, ***H***, Angular orientation of dendritic initiation sites of control (***G***) and FZD3-deficient neurons (***H***) 2 WPI. ***I***, Cumulative distribution plots of ***G*** and ***H*** (*$p < 0.05$, K–S test). ***J***, Representative images of 6-week-old GFP$^+$DCX$^+$ cells. GFP (green); DAPI (red). Scale bar, 50 μm. ***K***, Total dendritic length of 6-week-old GFP$^+$DCX$^+$ neurons (***$p < 0.001$, Student's *t* test). ***L***, Total number of intersections of 6-week-old GFP$^+$DCX$^+$ neurons (**$p < 0.01$, Student's *t* test).

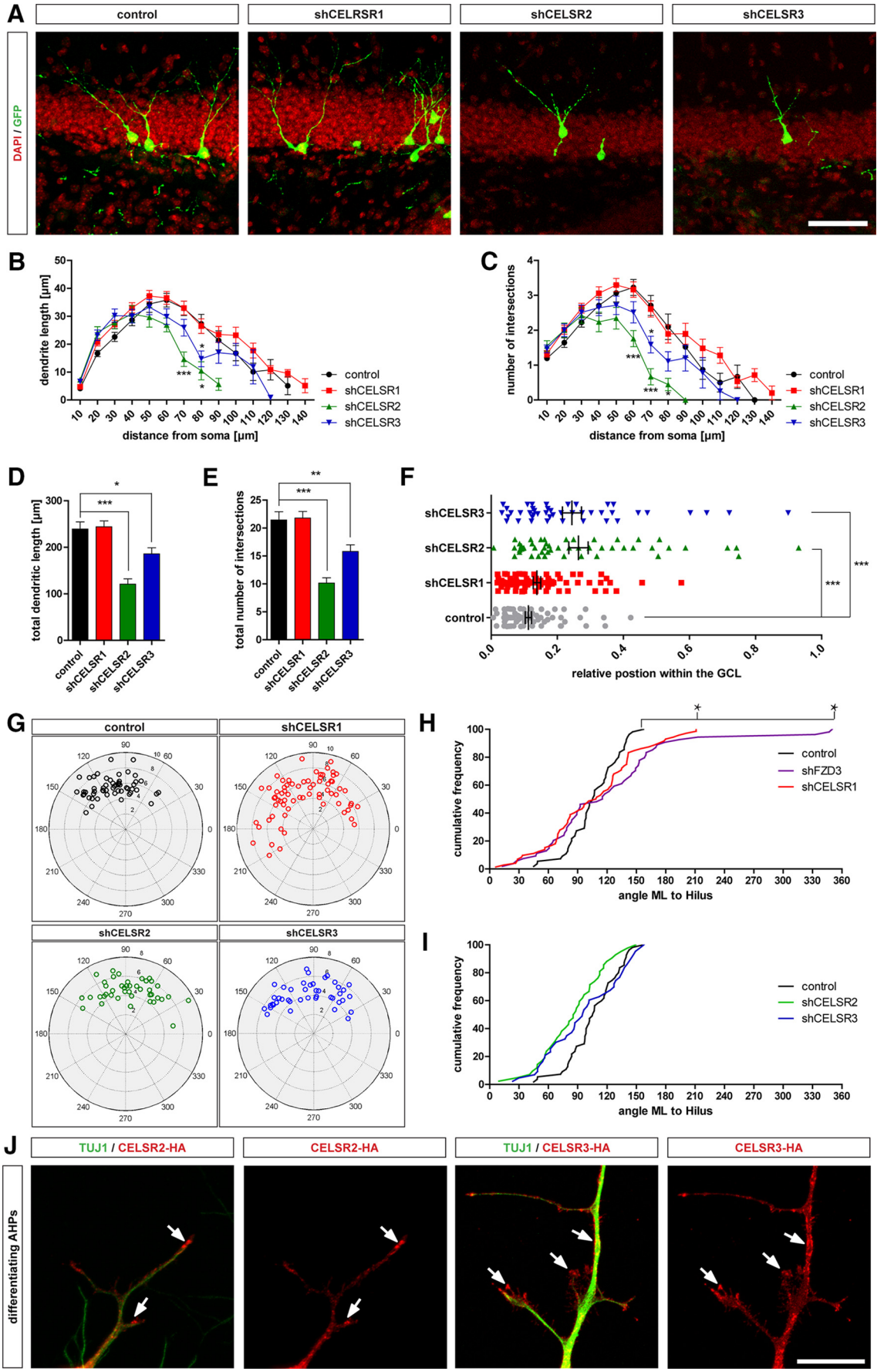
A
control
shCELRSR1
shCELSR2
shCELSR3
DAPI / GFP
B
dendrite length [µm]
distance from soma [µm]
control
shCELSR1
shCELSR2
shCELSR3
C
number of intersections
distance from soma [µm]
D
total dendritic length [µm]
E
total number of intersections
F
relative postion within the GCL
G
H
cumulative frequency
angle ML to Hilus
shFZD3
I
J
TUJ1 / CELSR2-HA
CELSR2-HA
TUJ1 / CELSR3-HA
CELSR3-HA
differentiating AHPs

stronger shRNA (shATP6AP2 #2), we found a much stronger reduction in cells that became DCX$^+$. This finding could be due to the fact that they had a more pronounced reduction in canonical Wnt signaling, which has been shown to regulate the differentiation of adult NSCs toward the neuronal lineage (Song et al., 2002; Lie et al., 2005; Gao et al., 2009; Kuwabara et al., 2009; Lavado et al., 2010; Karalay et al., 2011). In addition, LRP6 and LEF1 have been shown to play a pivotal role in dentate granule cell production during development (Zhou et al., 2004), and nuclear β-catenin through the TCF/LEF pathway does not affect dendritogenesis in cultured hippocampal neurons (Rosso et al., 2005). In-line with these studies, knockdown of LRP6 in adult hippocampal progenitors resulted in reduced levels of neurogenesis but did not affect granule cell morphogenesis, suggesting that canonical Wnt signaling mainly regulates proliferation and cell-fate determination of adult NSCs.

In striking contrast to the role of Wnt/β-catenin signaling in early steps of adult neurogenesis, we identified the Wnt/PCP signaling pathway as being a novel regulator of morphological development once neuronal cell fate had been determined. Wnt/PCP signaling is involved in converting signals into morphogenic programs and has essential functions in dendritic patterning, axonal tract development, neuronal migration, and hair cell orientation (Tissir and Goffinet, 2013). We found that Wnt/PCP signaling did not appear to be involved in early steps of adult neurogenesis, because knockdown of the PCP core protein FZD3 did not affect neuronal cell fate. FZD3 had been reported to be strongly expressed in the soma, axon, and dendrites of hippocampal neurons (Davis et al., 2008). Major axon tracts, such as the internal capsule and the anterior commissure, are absent in FZD3 knock-out mice, whereas the hippocampal system and several other axonal pathways are normal (Tissir et al., 2005). Recent work has shown that the FZD3-CELSR system controls facial branchiomotor (FBM) neuron migration (Qu et al., 2010), and several reports have revealed crucial roles for CELSR1-3 in many aspects of neuronal morphogenesis (Feng et al., 2012a). We found that silencing FZD3 in adult-born granule cells caused severe defects in dendritic growth, migration, and dendrite orientation. Compellingly, the phenotype of ATP6AP2-deficient cells that are committed to neuronal cell fate closely resembles that of shFZD3-expressing granule cells. This resemblance could be because the Wnt/PCP signaling pathway plays an important role during this major morphogenic stage, thereby explaining the context-specific role of this newly discovered Wnt signaling adaptor protein. At this stage, we cannot rule out the possibility that ATP6AP2 interferes with other signaling pathways. However, the striking phenotypic similarities, the specific protein interactions with FZD3 and CELSR2, 3 (CELSR1 also reported by Hermle et al., 2013), and the effect of ATP6AP2 on the signaling response point to a direct involvement of ATP6AP2 in PCP signaling during granule cell morphogenesis. With regard to the stage-specific role of Wnt/PCP signaling, further analyses are needed to specify the mechanisms that mediate the maturational transition of Wnt signaling responsiveness.

We further characterized distinctive morphogenic functions of the Wnt/PCP core proteins CELSR1-3 in granule cell maturation. Knockdown of CELSR1 affected cell orientation within the GCL, whereas CELSR2 and CELSR3 knockdowns resulted in reduced dendritic growth and abnormal cell migration, consistent with findings for CELSR1 in hair follicle cells, where it is necessary for a proper orientation (Devenport and Fuchs, 2008). Additionally, CELSR2 and 3 have been shown to control the ability of FBM neurons to migrate, whereas CELSR1 contributes to specifying the migratory direction (Qu et al., 2010).

The expression pattern of CELSR genes further supports the idea that CELSR1, CELSR2, and CELSR3 have divergent functions in mammals. During development CELSR1 is mostly expressed in neuroblasts and CELSR2 and 3 mainly in postmitotic neurons (Formstone and Little, 2001; Shima et al., 2002; Tissir et al., 2002; Tissir and Goffinet, 2006, 2013). The gene expression of CELSRs in differentiating AHPs revealed an overall upregulation of CELSR1-3. Nevertheless, CELSR1 expression levels showed a much more pronounced upregulation during the early differentiation steps, which could be because CELSR1 is required earlier to orient adult-born neuroblasts.

Downregulation of CELSR2 has been shown to reduce the length of dendrites in cultured cortical pyramidal neurons, whereas silencing of CELSR3 led to dendritic overgrowth (Shima et al., 2007). In contrast, pyramidal neurons of the cornu ammonis 1 (CA1) in CELSR3 mutant mice had atrophic dendritic trees and a reduced dendritic complexity (Feng et al., 2012b). We found that silencing of CELSR2 and 3 led to reduced dendritic growth and less complex dendritic trees in newborn granule cells *in vivo*. In their study, Shima et al. (2007) also demonstrated that the effect of CELSR3 on dendritic growth is dependent on the concentration of the applied molecule itself. Higher concentrations of CELSR3 stimulated dendritic growth in the same way as CELSR2. Because interactions of CELSR proteins are thought to be homophilic, their action on individual cells might be related to the environmental CELSR expression. Based on the phenotypic similarities of CELSR2 and 3 silencing in adult-born granule cells, we speculate that the environmental properties of the DG may cause the regulation of dendritic growth in the same way. Consistent with their function in dendritic patterning, CELSR2 and 3 appear to be expressed in the membrane of elongating neurites and particularly enriched in the tips of filopodia in differentiating AHPs *in vitro*.

It would be interesting to further characterize local cues upstream of PCP that could align cell polarity along a given local axis. Recent studies showing that the soluble Wnt inhibitor sFRP3 is involved in dentate granule cell maturation could point to Wnt ligands as modulators of non-canonical signaling (Jang et al., 2013). However, further studies are needed to provide evidence for a Wnt ligand-dependent non-canonical pathway in the DG.

In summary, the data presented here characterize a maturational transition of Wnt signaling responsiveness from Wnt/β-

←

Figure 9. Single-gene knockdowns of CELSR1-3 reveal distinctive morphogenic properties cooperatively resembling those of FZD3-deficient neurons. ***A***, Representative images of 2-week-old control shRNA- and shCELSR1-3-expressing neurons. DAPI (red); GFP (green). Scale bar, 50 μm. ***B***, Sholl analysis of the dendritic length of the PCP mutants shCELSR1-3. The data represent mean ± SEM (number of traced neurons: control: $n = 53$; shCELSR1: $n = 68$; shCESLR2: $n = 49$; shCESLR3: $n = 45$. $^*p < 0.05$, $^{***}p < 0.001$, Student's t test). ***C***, Sholl analysis of the dendritic complexity of the PCP mutants shCELSR1-3 (same groups of cells as in ***B*** were analyzed; $^*p < 0.05$, $^{**}p < 0.01$, $^{***}p < 0.001$, Student's t test). ***D***, Total dendritic length of GFP$^+$DCX$^+$ neurons 2 WPI ($^{**}p < 0.01$, Student's t test). ***E***, Total number of intersections of GFP$^+$DCX$^+$ neurons 2 WPI ($^*p < 0.05$, $^{**}p < 0.01$, Student's t test). ***F***, Relative positions of CELSR1-3-deficient neurons within the GCL ($^{***}p < 0.001$, Student's t test). ***G***, Angular orientation of dendritic initiation sites of control and CELSR1-3-deficient neurons 2 WPI. ***H***, ***I***, Cumulative distribution plots of ***G*** ($^*p < 0.05$, K–S test). ***J***, Neurite structures of AHP-derived neuroblasts *in vitro*. The subcellular localization of CELSR2 and 3 (red) in neurite structures (arrows) is shown using an HA-tagged overexpression construct. TUJ1 (green), CELS2-HA, and CELSR3-HA (red). Scale bar, 20 μm.

catenin signaling to non-canonical Wnt/PCP signaling in the course of adult hippocampal neurogenesis. Our findings suggest that these pathways show stage-dependent activities and regulate distinct steps of dentate granule cell neurogenesis. We provide conclusive evidence of a regulation of granule cell morphogenesis through the Wnt/PCP signaling pathway, including the FZD3-CELSR1-3 system.

References

Alvarez-Buylla A, Lim DA (2004) For the long run: maintaining germinal niches in the adult brain. Neuron 41:683–686. CrossRef Medline

Bilic J, Huang YL, Davidson G, Zimmermann T, Cruciat CM, Bienz M, Niehrs C (2007) Wnt induces LRP6 signalosomes and promotes dishevelled-dependent LRP6 phosphorylation. Science 316:1619–1622. CrossRef Medline

Blitzer JT, Nusse R (2006) A critical role for endocytosis in Wnt signaling. BMC Cell Biol 7:28. CrossRef Medline

Buechling T, Bartscherer K, Ohkawara B, Chaudhary V, Spirohn K, Niehrs C, Boutros M (2010) Wnt/frizzled signaling requires dPRR, the *Drosophila* homolog of the prorenin receptor. Curr Biol 20:1263–1268. CrossRef Medline

Cruciat CM, Ohkawara B, Acebron SP, Karaulanov E, Reinhard C, Ingelfinger D, Boutros M, Niehrs C (2010) Requirement of prorenin receptor and vacuolar H+-ATPase-mediated acidification for Wnt signaling. Science 327:459–463. CrossRef Medline

Davis EK, Zou Y, Ghosh A (2008) Wnts acting through canonical and non-canonical signaling pathways exert opposite effects on hippocampal synapse formation. Neural Dev 3:32. CrossRef Medline

Devenport D, Fuchs E (2008) Planar polarization in embryonic epidermis orchestrates global asymmetric morphogenesis of hair follicles. Nat Cell Biol 10:1257–1268. CrossRef Medline

Feng J, Han Q, Zhou L (2012a) Planar cell polarity genes, Celsr1-3, in neural development. Neurosci Bull 28:309–315. CrossRef Medline

Feng J, Xu Y, Wang M, Ruan Y, So KF, Tissir F, Goffinet A, Zhou L (2012b) A role for atypical cadherin Celsr3 in hippocampal maturation and connectivity. J Neurosci 32:13729–13743. CrossRef Medline

Formstone CJ, Little PF (2001) The flamingo-related mouse Celsr family (Celsr1-3) genes exhibit distinct patterns of expression during embryonic development. Mech Dev 109:91–94. CrossRef Medline

Gage FH (2000) Mammalian neural stem cells. Science 287:1433–1438. CrossRef Medline

Galceran J, Miyashita-Lin EM, Devaney E, Rubenstein JL, Grosschedl R (2000) Hippocampus development and generation of dentate gyrus granule cells is regulated by LEF1. Development 127:469–482. Medline

Gao Z, Ure K, Ables JL, Lagace DC, Nave KA, Goebbels S, Eisch AJ, Hsieh J (2009) Neurod1 is essential for the survival and maturation of adult-born neurons. Nat Neurosci 12:1090–1092. CrossRef Medline

Garbe DS, Ring RH (2012) Investigating tonic Wnt signaling throughout the adult CNS and in the hippocampal neurogenic niche of BatGal and ins-TopGal mice. Cell Mol Neurobiol 32:1159–1174. CrossRef Medline

Ge S, Yang CH, Hsu KS, Ming GL, Song H (2007) A critical period for enhanced synaptic plasticity in newly generated neurons of the adult brain. Neuron 54:559–566. CrossRef Medline

Hermle T, Guida MC, Beck S, Helmstädter S, Simons M (2013) *Drosophila* ATP6AP2/VhaPRR functions both as a novel planar cell polarity core protein and a regulator of endosomal trafficking. EMBO J 32:245–259. CrossRef Medline

Jang MH, Bonaguidi MA, Kitabatake Y, Sun J, Song J, Kang E, Jun H, Zhong C, Su Y, Guo JU, Wang MX, Sailor KA, Kim JY, Gao Y, Christian KM, Ming GL, Song H (2013) Secreted frizzled-related protein 3 regulates activity-dependent adult hippocampal neurogenesis. Cell Stem Cell 12:215–223. CrossRef Medline

Jessberger S, Aigner S, Clemenson GD Jr, Toni N, Lie DC, Karalay O, Overall R, Kempermann G, Gage FH (2008) Cdk5 regulates accurate maturation of newborn granule cells in the adult hippocampus. PLoS Biol 6:e272. CrossRef Medline

Jessberger S, Clark RE, Broadbent NJ, Clemenson GD Jr, Consiglio A, Lie DC, Squire LR, Gage FH (2009) Dentate gyrus-specific knockdown of adult neurogenesis impairs spatial and object recognition memory in adult rats. Learn Mem 16:147–154. CrossRef Medline

Karalay O, Doberauer K, Vadodaria KC, Knobloch M, Berti L, Miquelajauregui A, Schwark M, Jagasia R, Taketo MM, Tarabykin V, Lie DC, Jessberger S (2011) Prospero-related homeobox 1 gene (Prox1) is regulated by canonical Wnt signaling and has a stage-specific role in adult hippocampal neurogenesis. Proc Natl Acad Sci U S A 108:5807–5812. CrossRef Medline

Kuwabara T, Hsieh J, Muotri A, Yeo G, Warashina M, Lie DC, Moore L, Nakashima K, Asashima M, Gage FH (2009) Wnt-mediated activation of NeuroD1 and retro-elements during adult neurogenesis. Nat Neurosci 12:1097–1105. CrossRef Medline

Lavado A, Lagutin OV, Chow LM, Baker SJ, Oliver G (2010) Prox1 is required for granule cell maturation and intermediate progenitor maintenance during brain neurogenesis. PLoS Biol 8:e1000460. CrossRef Medline

Lie DC, Colamarino SA, Song HJ, Désiré L, Mira H, Consiglio A, Lein ES, Jessberger S, Lansford H, Dearie AR, Gage FH (2005) Wnt signalling regulates adult hippocampal neurogenesis. Nature 437:1370–1375. CrossRef Medline

Ming GL, Song H (2011) Adult neurogenesis in the mammalian brain: significant answers and significant questions. Neuron 70:687–702. CrossRef Medline

Niehrs C (2012) The complex world of WNT receptor signalling. Nat Rev Mol Cell Biol 13:767–779. CrossRef Medline

Palmer TD, Takahashi J, Gage FH (1997) The adult rat hippocampus contains primordial neural stem cells. Mol Cell Neurosci 8:389–404. CrossRef Medline

Pino D, Choe Y, Pleasure SJ (2011) Wnt5a controls neurite development in olfactory bulb interneurons. ASN Neuro 3:e00059. CrossRef Medline

Qu Y, Glasco DM, Zhou L, Sawant A, Ravni A, Fritzsch B, Damrau C, Murdoch JN, Evans S, Pfaff SL, Formstone C, Goffinet AM, Chandrasekhar A, Tissir F (2010) Atypical cadherins Celsr1-3 differentially regulate migration of facial branchiomotor neurons in mice. J Neurosci 30:9392–9401. CrossRef Medline

Ring L, Neth P, Weber C, Steffens S, Faussner A (2014) β-Catenin-dependent pathway activation by both promiscuous "canonical" WNT3a-, and specific "noncanonical" WNT4- and WNT5a-FZD receptor combinations with strong differences in LRP5 and LRP6 dependency. Cell Signal 26:260–267. CrossRef Medline

Rosso SB, Sussman D, Wynshaw-Boris A, Salinas PC (2005) Wnt signaling through Dishevelled, Rac and JNK regulates dendritic development. Nat Neurosci 8:34–42. CrossRef Medline

Schäfer ST, Peters J, von Bohlen Und Halbach O (2013) The (pro)renin receptor/ATP6ap2 is expressed in the murine hippocampus by adult and newly generated neurons. Restor Neurol Neurosci 31:225–231. CrossRef Medline

Schlessinger K, Hall A, Tolwinski N (2009) Wnt signaling pathways meet Rho GTPases. Genes Dev 23:265–277. CrossRef Medline

Shelly M, Lim BK, Cancedda L, Heilshorn SC, Gao H, Poo MM (2010) Local and long-range reciprocal regulation of cAMP and cGMP in axon/dendrite formation. Science 327:547–552. CrossRef Medline

Shima Y, Copeland NG, Gilbert DJ, Jenkins NA, Chisaka O, Takeichi M, Uemura T (2002) Differential expression of the seven-pass transmembrane cadherin genes Celsr1-3 and distribution of the Celsr2 protein during mouse development. Dev Dyn 223:321–332. CrossRef Medline

Shima Y, Kawaguchi SY, Kosaka K, Nakayama M, Hoshino M, Nabeshima Y, Hirano T, Uemura T (2007) Opposing roles in neurite growth control by two seven-pass transmembrane cadherins. Nat Neurosci 10:963–969. CrossRef Medline

Song H, Stevens CF, Gage FH (2002) Astroglia induce neurogenesis from adult neural stem cells. Nature 417:39–44. CrossRef Medline

Tissir F, Goffinet AM (2006) Expression of planar cell polarity genes during development of the mouse CNS. Eur J Neurosci 23:597–607. CrossRef Medline

Tissir F, Goffinet AM (2013) Shaping the nervous system: role of the core planar cell polarity genes. Nat Rev Neurosci 14:525–535. CrossRef Medline

Tissir F, De-Backer O, Goffinet AM, Lambert de Rouvroit C (2002) Developmental expression profiles of Celsr (Flamingo) genes in the mouse. Mech Dev 112:157–160. CrossRef Medline

Tissir F, Bar I, Jossin Y, De Backer O, Goffinet AM (2005) Protocadherin

Celsr3 is crucial in axonal tract development. Nat Neurosci 8:451–457. CrossRef Medline

van Amerongen R, Nusse R (2009) Towards an integrated view of Wnt signaling in development. Development 136:3205–3214. CrossRef Medline

van Praag H, Schinder AF, Christie BR, Toni N, Palmer TD, Gage FH (2002) Functional neurogenesis in the adult hippocampus. Nature 415:1030–1034. CrossRef Medline

von Bohlen und Halbach O (2011) Immunohistological markers for proliferative events, gliogenesis, and neurogenesis within the adult hippocampus. Cell Tissue Res 345:1–19. CrossRef Medline

Wang C, Zhao Y, Su Y, Li R, Lin Y, Zhou X, Ye L (2013) C-Jun N-terminal kinase (JNK) mediates Wnt5a-induced cell motility dependent or independent of RhoA pathway in human dental papilla cells. PLoS One 8:e69440. CrossRef Medline

Yamamoto H, Komekado H, Kikuchi A (2006) Caveolin is necessary for Wnt-3a-dependent internalization of LRP6 and accumulation of beta-catenin. Dev Cell 11:213–223. CrossRef Medline

Yamanaka H, Moriguchi T, Masuyama N, Kusakabe M, Hanafusa H, Takada R, Takada S, Nishida E (2002) JNK functions in the non-canonical Wnt pathway to regulate convergent extension movements in vertebrates. EMBO Rep 3:69–75. CrossRef Medline

Yuan JS, Reed A, Chen F, Stewart CN Jr (2006) Statistical analysis of real-time PCR data. BMC Bioinformatics 7:85. CrossRef Medline

Zhao C, Teng EM, Summers RG Jr, Ming GL, Gage FH (2006) Distinct morphological stages of dentate granule neuron maturation in the adult mouse hippocampus. J Neurosci 26:3–11. CrossRef Medline

Zhou CJ, Zhao C, Pleasure SJ (2004) Wnt signaling mutants have decreased dentate granule cell production and radial glial scaffolding abnormalities. J Neurosci 24:121–126. CrossRef Medline